
KADIR HAS UNIVERSITY
SCHOOL OF GRADUATE STUDIES
PROGRAM OF ELECTRONICS ENGINEERING

# DIVERSITY TECHNIQUES FOR SPARSE CODE MULTIPLE ACCESS

OĞUZ ÜLGEN

DOCTOR OF PHILOSOPHY THESIS

ISTANBUL, NOVEMBER, 2024

# DIVERSITY TECHNIQUES FOR SPARSE CODE MULTIPLE ACCESS

OĞUZ ÜLGEN

A thesis submitted to
the School of Graduate Studies of Kadir Has University
in partial fulfilment of the requirements for the degree of
Doctor of Philosophy in
Electronics Engineering

İstanbul, November, 2024

# APPROVAL

This thesis titled DIVERSITY TECHNIQUES FOR SPARSE CODE MULTIPLE ACCESS submitted by OĞUZ ÜLGEN, in partial fulfillment of the requirements for the degree of Doctor of Philosophy in Electronics Engineering is approved by

Assoc. Prof. Dr. Tunçer Baykaş (Advisor) .....
Kadir Has University

Prof. Dr. Serhan Yarkan .....
Istanbul Ticaret University

Prof. Dr. Mehmet Timur Aydemir .....
Kadir Has University

Asst. Prof. Dr. Çağatay Edemen .....
Özyegin University

Asst. Prof. Dr. Yalçın Şadi .....
Kadir Has University

I confirm that the signatures above belong to the aforementioned faculty members.

.....
Prof. Dr. Mehmet Timur Aydemir
Dean of School of Graduate Studies
Date of Approval: .....

## DECLARATION ON RESEARCH ETHICS AND PUBLISHING METHODS

I, OĞUZ ÜLGEN; hereby declare

- that this Ph.D. Thesis that I have submitted is entirely my own work and I have cited and referenced all material and results that are not my own in accordance with the rules;
- that this Ph.D. Thesis does not contain any material from any research submitted or accepted to obtain a degree or diploma at another educational institution;
- and that I commit and undertake to follow the "Kadir Has University Academic Codes and Conduct" prepared in accordance with the "Higher Education Council Codes of Conduct".

In addition, I acknowledge that any claim of irregularity that may arise in relation to this work will result in a disciplinary action in accordance with university legislation.

OĞUZ ÜLGEN

. . . . . .

.....

To the scientists who sacrificed their lives in the pursuit of knowledge

# ACKNOWLEDGEMENT

I would like to express my appreciation to my thesis supervisor Dr. Tunçer Bayka¸s. Without his guidance and knowledge, I would not be able to complete my PhD. I would also like to thank Dr. Serhat Erkü çü k, with whom I have been working together for 8 years. He is the one who has convinced me to take part in the research area and start this journey with a master's study in 2016.

I would also like to thank Dr. Yalçın Şadi for his feedback on my research work. His vision motivated me a lot through my research.

I would like to thank my friends for their understanding.

Last but not least, I would like to express my thankfulness to my family. The unconditional support of them gave me the strength to carry out my thesis and to finish it.

Important note: This work was supported by the Scientific and Technological Research Council Of Türkiye (TÜ BI˙TAK) under Grant 120E496.

# ABSTRACT

The main objectives of the next-generation wireless communication systems are to improve spectral efficiency and increase data rates. While traditional wireless systems usually rely on Orthogonal Multiple Access (OMA) techniques, non-orthogonal multiple access (NOMA) is introduced in 5G as a new paradigm. NOMA is a promising solution to meet the increased demands of the future wireless communication networks. One of the NOMA methods is Sparse Code Multiple Access (SCMA). SCMA offers diversity gains through signal constellation coding. However, research on optimizing the performance of SCMA is limited, especially in the diversity components. This PhD thesis proposes a novel multiple-access model. This model implements various diversity techniques for downlink SCMA. The proposed model's performance is evaluated through both computer simulations and mathematical analysis. To further enhance this model, advanced diversity combining techniques are integrated, including evolution-based metaheuristic algorithms. Given the increased complexity of the new model, a complexity analysis is also conducted. Finally, comparative demonstrations show the superiority of the proposed model over traditional SCMA and how the diversity components affect the performance results. The results highlight the potential of the proposed model for future wireless communication systems.

**Keywords: Wireless Communication Networks, Non-Orthogonal Multiple Access, Sparse Code Multiple Access, Diversity Combining Techniques, Evolution-Based Metaheuristic Algorithms**

# ÖZET

Gelecek nesil kablosuz iletişim sistemlerinin ana hedefleri, spektral verimliliği artırmak ve veri hızlarını yükseltmektir. Geleneksel kablosuz sistemler genellikle Ortogonal Çoklu Erişim (OMA) tekniklerine dayanırken, 5G'de yeni bir paradigma olarak ortogonal olmayan çoklu erişim (NOMA) tanıtılmıştır. NOMA, gelecekteki kablosuz iletişim ağlarının artan taleplerini karşılamak için umut verici bir çözüm sunmaktadır. NOMA yöntemlerinden biri olan Seyrek Kodlu Çoklu Erişim (SCMA), sinyal konstelasyon kodlaması yoluyla çeşitlilik kazançları sağlar. Ancak, SCMA'nın performansını optimize etmeye yönelik araştırmalar sınırlıdır, özellikle çeşitlilik bileşenlerinde. Bu doktora tezi, yeni bir çoklu erişim modeli önermektedir. Bu model, downlink SCMA için çeşitli çeşitlilik tekniklerini uygular. Önerilen modelin performansı, hem bilgisayar simülasyonları hem de matematiksel analizler yoluyla değerlendirilmektedir. Bu modeli daha da geliştirmek için, evrim tabanlı meta-sezgisel algoritmalar dahil olmak üzere gelişmiş çeşitlilik birleştirme teknikleri entegre edilmiştir. Yeni modelin artan karmaşıklığı göz önünde bulundurularak bir karmaşıklık analizi de yapılmaktadır. Son olarak, karşılaştırmalı gösterimler, önerilen modelin geleneksel SCMA'ya göre üstünlüğünü ve çeşitlilik bileşenlerinin performans sonuçlarını nasıl etkilediğini göstermektedir. Sonuçlar, önerilen modelin gelecekteki kablosuz iletişim sistemleri için potansiyelini vurgulamaktadır.

**Anahtar Sözcükler: Kablosuz İletişim Ağları, Dikgen Olmayan Çoklu Erişim, Seyrek Kodlu Çoklu Erişim, Çeşitlemeli Birleştirme Teknikleri, Evrim Tabanlı Meta-Sezgisel Algoritmalar**

# TABLE OF CONTENTS

# LIST OF FIGURES

# LIST OF TABLES

# LIST OF SYMBOLS

| | |
|---|---|
| Ap | A priori probability |
| $c_i$ | Pseudo-random code for the given user i |
| $C_j$ | Constellation matrix for user j |
| d | Data signal |
| $d'$ | Decoded data signal |
| $e^{(M)}$ | Unit vector with dimension M |
| $f_{ML}$ | Non-linear function for maximum likelihood detection |
| $f_{MPA}$ | Non-linear function for message passing algorithm |
| **F** | Factor graph matrix |
| **J** | Number of users |
| K | Number of sub-carriers |
| M | Modulation order |
| n | Noise component |
| $P_{e,s}$ | Probability of symbol error |
| r | Received signal |
| R | Total received signal for the system |
| s | Transmitted signal |
| $s_d$ | Modulated data bits |
| $s'$ | Decoded transmitted signal |
| S | Total transmitted signal for the system |
| **Q** | Q function |
| $V_j$ | Mapping matrix for user j |
| $Z_N$ | N-dimensional integer matrix space |
| R | Rational matrix space |
| $\lceil \cdot \rceil$ | Ceiling function |
| $\lfloor \cdot \rfloor$ | Floor function |
| $\circ$ | Hadamard product |

# LIST OF ACRONYMS AND ABBREVIATIONS

| | |
|---|---|
| BER | Bit-Error Rate |
| CDMA | Code-Division Multiple Access |
| CD-NOMA | Code-Domain Non-Orthogonal Multiple Access |
| EGC | Equal Gain Combining |
| FN | Function Node |
| GA | Genetic Algorithm |
| ICA | Imperialist Competitive Algorithm |
| IDMA | Interleave Division Multiple Access |
| IGMA | Interleave-Grid Multiple Access |
| LDS | Low-Density Signature |
| LDS-CDMA | Low-Density Spreading Code-Division Multiple Access |
| LDS-OFDM | Low-density Signature Orthogonal Frequency Division Multiplexing |
| LLR | Log-likelihood Ratio |
| MIMO | Multiple-input and Multiple-output |
| MPA | Message Passing Algorithm |
| MRC | Maximum Ratio Combining |
| MUSA | Multi-user Shared Access |
| NOCA | Non-Orthogonal Coded Access |
| NOMA | Non-Orthogonal Multiple Access |
| OFDMA | Orthogonal Frequency Division Multiple Access |
| OMA | Orthogonal Multiple Access |
| OVSF | Orthogonal Variable Spreading Factor |
| PD-NOMA | Power-Domain Non-Orthogonal Multiple Access |
| PDMA | Pattern Division Multiple Access |
| SAMA | Successive Interference Cancellation Amenable Multiple Access |
| SC | Selection Combining |
| SCMA | Sparse Code Multiple Access |
| SCMA-RT | Sparse Code Multiple Access with Repetitive Transmission |
| SCMA-TS | Sparse Code Multiple Access with Time-Spreading |

| | |
|---|---|
| SCMA-TSRT | SCMA with Time-Spreading and Repetitive Transmission |
| SER | Symbol Error Rate |
| SIC | Successive Interference Cancellation |
| SF | Spreading Factor |
| SNR | Signal-to-Noise Ratio |
| VN | Variable Node |

# 1. INTRODUCTION

Wireless communication has been a part of daily life since the beginning of humanity. Communication with mirrors, smoke signals, or beacon fires was the ancient type of it. Throughout history, many technologies have been developed to further increase the effectiveness of wireless communication. Advanced technologies such as electromagnetic signaling and mobile phones are now the key elements of the everyday. People, through mobile phones and other digital devices, transmit and receive hundreds of millions of bits daily, and the number of users is increasing rapidly. These advancements are bringing new problems with them. Since the resource of wireless communication is the frequency spectrum, physical limitations are pushing researchers to find new ways to use the spectrum efficiently [1].

One recently introduced technology is sparse code multiple access (SCMA). [2] first introduced this technique to further increase the spectral efficiency of new-generation wireless communication technologies. The following section will give an overview of SCMA and the motivation for focusing on it. Then, the contribution of the thesis will be presented, followed by the organization of the dissertation.

## 1.1 Motivation for Sparse Code Multiple Access

In the 5G cellular communication standards, there are two main multiple access techniques used, which are orthogonal multiple access or, more specifically, Orthogonal Frequency Division Multiple Access (OFDMA) and Non-Orthogonal Multiple Access (NOMA). OFDMA has been used for 4G systems as well. However, NOMA is a more recent technology, and it promises better spectral efficiency by letting users use the same time and frequency resources via implementing novel interference cancellation methods [3].

The NOMA techniques can be categorized into two main categories: Power-domain NOMA (PD-NOMA) and code-domain NOMA (CD-NOMA). There are several works to compare PD-NOMA and CD-NOMA in various ways [4], [5]. These studies have shown that CD-NOMA performs better than PD-NOMA in terms of sum rate. Since the demand for higher data rates must be satisfied in future communication networks, CD-NOMA can be considered as a better alternative.

Researchers have studied several different CD-NOMA techniques. Low-Density Signature (LDS), Interleave Division Multiple Access (IDMA), Pattern Division Multiple Access (PDMA), and Interleave-Grid Multiple Access (IGMA) are some examples. However, when compared with the other techniques, Sparse Code Multiple Access (SCMA) stands out with its novel transmitter and receiver coding schemes [6].

As a pioneering approach for SCMA [7], Nikopour and Baligh have proposed a scheme where, in the transmitter, the pre-encoded data bits are transferred to SCMA spreading encoder to be assigned to sparse codewords. At the receiver, the message-passing algorithm (MPA) technique is applied to decode these SCMA-encoded bits, and the model is accepted as the traditional SCMA model.

In earlier studies there are some approaches to further investigate the variables of the SCMA systems. In study [8], different codebook designs are compared. In study [9], system overload effects are investigated by adjusting the number of users or the number of carriers. [10] shows the effect of using different number of users in the SCMA systems. The current studies mainly concentrate on the design of the codebook or the system overload mostly. There is limited research on new spreading models and transmission techniques. Therefore, this thesis explores diversity techniques of SCMA, including time-spreading and repetitive transmission, as well as related sub-techniques.

## 1.2 Contribution

In this thesis, the effects of the addition of time-spreading and repetitive transmission to the SCMA systems are investigated. Additionally, a new model to use time-spreading and repetitive transmissions for downlink SCMA is proposed. The following contributions are presented further:

1. Integration details of the repetitive transmissions and time-spreading for SCMA.
2. Theoretical upper bound analysis of the proposed model.
3. Complexity analysis of the proposed model.
4. Diversity combining techniques for the proposed model.
5. Further techniques investigated during the thesis studies.

## 1.3 Dissertation Organization

The dissertation consists of six chapters. The basic introduction to SCMA and the motivation behind the thesis are given in Chapter 1. Chapter 2 presents the background of SCMA and various diversity techniques in SCMA. Chapter 3 explains the details of the proposed model, SCMA with time-spreading and repetitive transmissions. In Chapter 4, diversity combining techniques on the proposed model is given. Chapter 5 presents the further results obtained during the preparation of the thesis. Finally, Chapter 6 concludes the thesis and proposes new possible study areas of the model for the future.

# 2. BACKGROUND

## 2.1 Non-Orthogonal Multiple Access

One of the biggest challenges faced by beyond 5G wireless networks is supporting large-scale mobile communication traffic. Accordingly, new multiple-access techniques are being developed to meet the demand. One of these techniques is NOMA. As mentioned in Chapter 1, NOMA has two sub-categories which are PD-NOMA and CD-NOMA. The next subsections introduce these concepts and explain the details.

### 2.1.1 Power Domain Non-Orthogonal Multiple Access

PD-NOMA basically allows multiple users to access the same frequency non-orthogonally by adjusting signal powers according to the channel conditions. Two key concepts of the technique are successive interference cancellation (SIC) at the receiver and superposition coding at the transmitter.

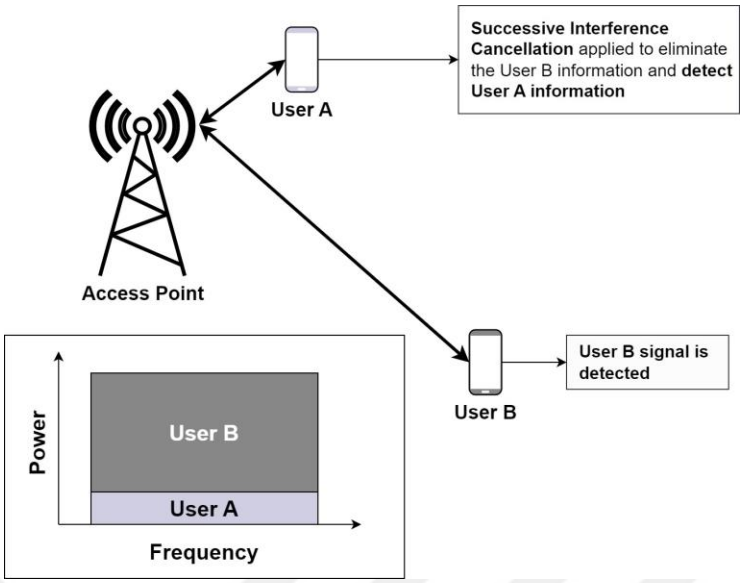


Figure 2.1: Signal detection in PD-NOMA for two users scenario.

Fundamentally, superposition coding of multiple signals is the key aspect that offers non-orthogonality. This means the signals of multiple users are combined and transmitted together. Power allocation is important to increase the chance of being detected by the right user. The user with a higher distance, in other words, the normalized channel gain is lower, is allocated with higher power, and the user with the lowest distance is allocated with low power. Multiplexing multiple users also requires superimposing the constellation diagrams of these users and adjusting the constellations accordingly.

SIC is the second fundamental concept of PD-NOMA. At the receiver, the superimposed signal is received by all users. To eliminate the other signals and have each user's correct signal, the optimal order of detection starts with the strongest user. The most power-allocated user's signal is detected first, and later, the lower ones eliminate the detected signal and decode the correct signal. The procedure with two users is depicted in Figure 2.1.

SIC is a relatively low-complexity decoding technique compared to MPA, which is presented in more detail in the following sections. However, it is inherently error-

prone. If the first user detects a signal with errors, the rest of the signals will be detected wrongly, leading to a collapse of the system. Therefore, the number of users in a PD-NOMA system is usually kept relatively low. The increased number of users in PD-NOMA brings some problems, such as increased signaling overhead, high packet transmission delays, and the need for complex optimization methods [11, 12, 13, 14].

In summary, PD-NOMA is a multiple-access technique for future generation of wireless networks. It addresses the demand for increasing mobile communication traffic. By using successive interference cancellation and superposition coding, PD-NOMA enables multiple users to share the same frequency resource non-orthogonally, therefore enhancing spectral efficiency. However, the technique faces several challenges, such as the limited number of users sustained due to inherent problems. CD-NOMA is an alternative that brings another stance into SCMA.

### 2.1.2 Code Domain Non-Orthogonal Multiple Access

CD-NOMA allows multiple users to access the same frequency-time resource without interference by using unique spreading sequences. Similar to PD-NOMA, users decode the signal to have the correct information. However, SIC is not able to be used in this scenario, and a more complex solution is needed. Therefore, MPA is offered to tackle this problem [15]. While increasing the complexity, MPA offers a reliable solution for the spreading sequences in CD-NOMA.

There are several CD-NOMA schemes in literature, and each is listed and detailed as follows.

*Low-Density Spreading Code-Division Multiple Access (LDS-CDMA)*: Firstly introduced by Hoshyar et al. [16], LDS-CDMA uses sparse quasi-orthogonal spreading sequences, in which each sequence is composed of time chips. The superimposed symbols are spread over time chips and transmitted. At the

receiver, the MPA is used to detect and decode the signal. LDS-CDMA has high complexity for multi-user detection.

*Multi-User Shared Access (MUSA)*: This technique is very similar to PD-NOMA with a little difference. Multiple users are grouped, and each group receives the signal non-orthogonally using different power schemes. SIC is used to eliminate intra-group signals, while inter-group sequences are set orthogonally [17].

*Successive Interference Cancellation Amenable Multiple Access (SAMA)*: SAMA offers diversity through grouping users based on the system signature matrix and iterative multi-user interference cancellation technique [18]. Iterative MPA is used to detect the signals for each user and, in a manner with each iteration, improves the detection of signals until it reaches the threshold iteration number or saturation based on the system design.

There are other CD-NOMA techniques such as low-density signature orthogonal frequency division multiplexing (LDS-OFDM) or hybrid multiple access [19, 20]. However, the most commonly used CD-NOMA technique is, as the main focus of this thesis, SCMA.

### 2.1.3 Other Non-Orthogonal Multiple Access Techniques

There are also other non-orthogonal multiple access techniques studied in literature. Pattern division multiple access (PDMA), which focuses on using specific codebooks and binary patterns to be selected to increase the diversity order for robust down-link performance [21]. Interleave division multiple access (IDMA) and interleave grid multiple access (IGMA) are other examples of NOMA [22, 23]. These two techniques are based on using bit-level interleaver and sparse symbol-level grid. Another example is Non-Orthogonal Coded Access (NOCA). NOCA is based on LTE, using low correlation sequences to transmit signals that spread over time and frequency domains [24].

## 2.2 Diversity applications in wireless communication

Time, space, or frequency-spreading is used in wireless communication as diversity applications to tackle interference, increase capacity, or increase the robustness of the system. The next subsections introduce time-spreading and frequency-spreading in detail.

### 2.2.1 Time-Spreading

Time-spreading, in special cases also called time-coding, is a method that spreads a signal over a given time frame by multiplying the signal with a given code to increase the quality of the transmission [25]. There are different techniques to spread the signal over time. However, the most common one is to use orthogonal time chips to multiply the signal and afterward decode it at the receiver. Figure 2.2 depicts a simple spread signal over different time frames with a chip code consisting of +1's and -1's. This method is also fundamental to code-division multiplexing (CDMA) [26].

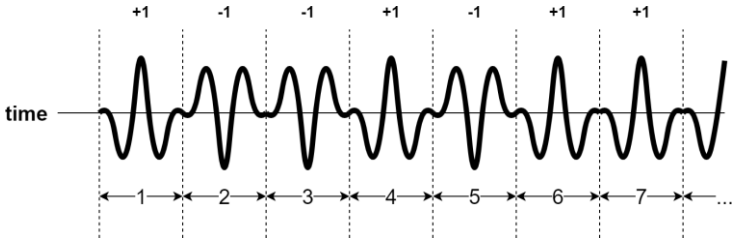


Figure 2.2: A signal spread over time with a chip code.

Assume the data to be transmitted for a single user is given as

$$d[t], \tag{2.1}$$

where t is the time variable. Data is converted to a signal through modulation techniques and becomes

$$s[t]. \tag{2.2}$$

Later, the signal of the user is assigned to a pseudo-random code C and becomes

$$s_k[t] \cdot c_k[t], \tag{2.3}$$

where k denotes the corresponding user, and $c_k$ is the corresponding chip value for the given spreading instance. The transmitted signal of the system is given as

$$S[t] = \sum_{k=1}^{K} s_k[t] \cdot c_k[t]. \tag{2.4}$$

For the received signal at the receiver, the pseudo-random code is used to decode the signal as follows

$$s'[t] = r_k[t] \cdot c_k[t], \tag{2.5}$$

where s′[t] is the decoded data and r[t] can be shown as

$$r_k[t] = s_k[t].c_k[t] + n[t], \tag{2.6}$$

where n is the noise component.

Basic transmitter and receiver block diagrams of the time-spreading system are given in Figure 2.3 and 2.4

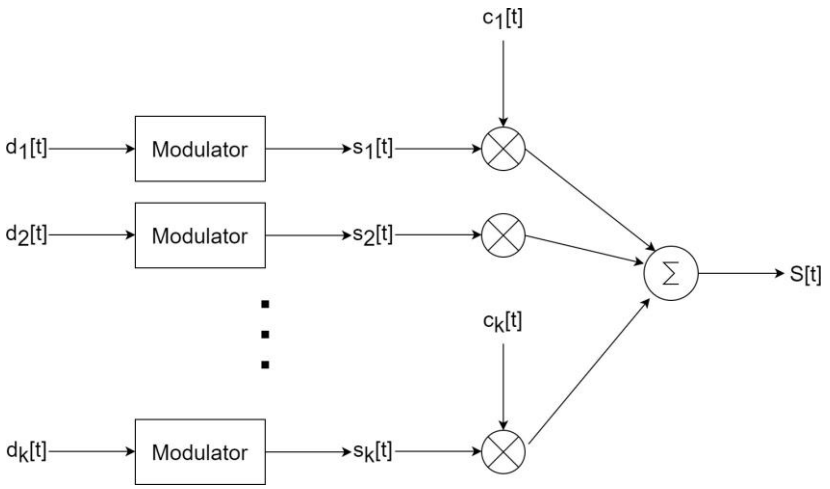


Figure 2.3: Basic transmitter block for time-spreading systems.

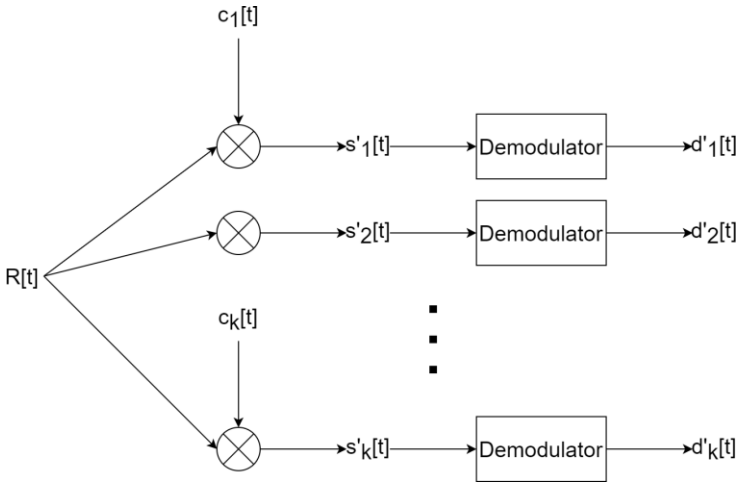


Figure 2.4: Basic receiver block for time-spreading systems.

The fundamentals of the time-spreading applications are kept the same in the system model, which is explained in the next chapters.

### 2.2.2 Frequency-Spreading

Frequency spreading is another diversity technique in wireless communication systems. The aim of the technique is to mitigate the possible shortcomings of the system due to interference in the frequency channels by dividing or multiplying the signal into multiple frequency channels at the transmitter and combining the signals at the receiver with the corresponding techniques [27]. A basic representation of the frequency-spreading is given in Figure 2.5. The dark gray resources are shown as used frequencies, and the white ones are free.

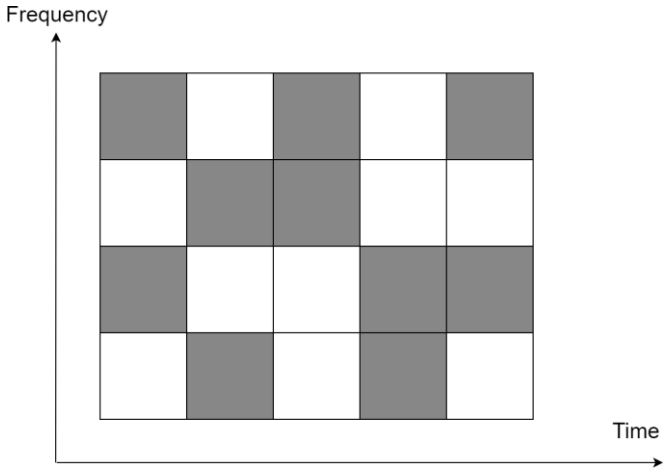


Figure 2.5: Basic representation of a frequency-spreading system using resource blocks.

Assume the data bits to be transmitted for a single user is given as

$$d(t), \tag{2.7}$$

where t is the time variable.

The bits are first modulated and later spread by using the frequency spreader block. Lastly the signal is transmitted as

$$s(t) = s_d(t) \times c(t), \tag{2.8}$$

where $s_d$ is the modulated data bits and c(t) is the carrier. The transmitter block is given in Figure 2.6.

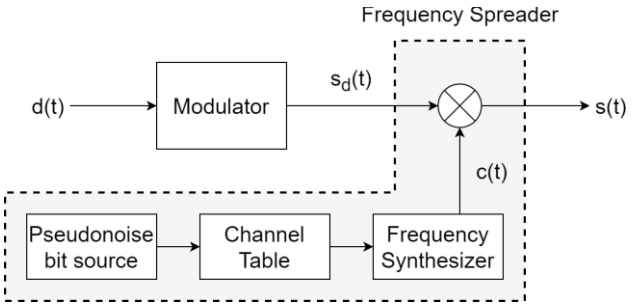


Figure 2.6: Basic transmitter block for frequency-spreading systems.

At the receiver, the signal is despreaded and demodulated to have the final signal as d′(t).

SCMA uses frequency-spreading inherently; therefore, the fundamentals of frequency-spreading are present in SCMA.

### 2.2.3 Other diversity techniques

Besides frequency and time-spreading, there are also other diversity techniques in the literature.

Space diversity is a technique used in multiple-input and multiple-output (MIMO) systems in wireless communication. Multiple antennas with spacing between are used to transmit a signal to create multiple paths and mitigate the possible issues in the channel.

A MIMO system with space diversity is shown in Figure 2.7. It is shown that two transmitters and two receivers have diverse channel communication and have multiple paths.

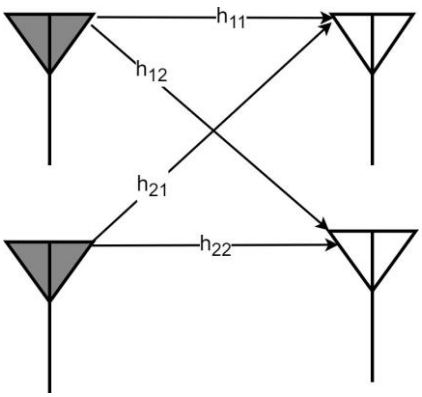


Figure 2.7: A simple MIMO space diversity system.

Another diversity technique is repetitive transmission, or repetition-coding. In repetitive transmission, similar to space diversity, the aim is to transmit a signal under different channel conditions. Instead of using antenna spacing, the time domain is used to transmit the data repetitively. Later, the signals received are combined at the receiver using different techniques. Assume the signal for a transmission period is $s_j[t]$. Then, the transmitted signal for a single information signal after u transmission is given as:

$$s'_j[t] = [s_{j,1}[t], s_{j,2}[t], ..., s_{j,u}[t]], \quad (2.9)$$

where $s'_j$ is the concatenation of u times repeated signal of $s_j$ and [...] denotes the concatenation. Since $s_j$ is repeated u times with the same characteristics, $s_{j,1}[b] = s_{j,2}[b] = ... = s_{j,u}[b]$. Assume the channel coefficients change with every transmission, then the received signal becomes

$$r'_j[t] = [r_{j,1}[t] \cdot h_1 + n_1, s_{j,2}[t] \cdot h_2 + n_2, ..., s_{j,u}[t] \cdot h_u + n_u], \quad (2.10)$$

where h denotes the channel gain coefficient and n is noise.

A basic repetitive transmission schema is given in Figure 2.8. In this schema, the spreading factor is 4. This means there are 4 repetitive transmissions for every information signal to be transmitted to the receiver to be combined.

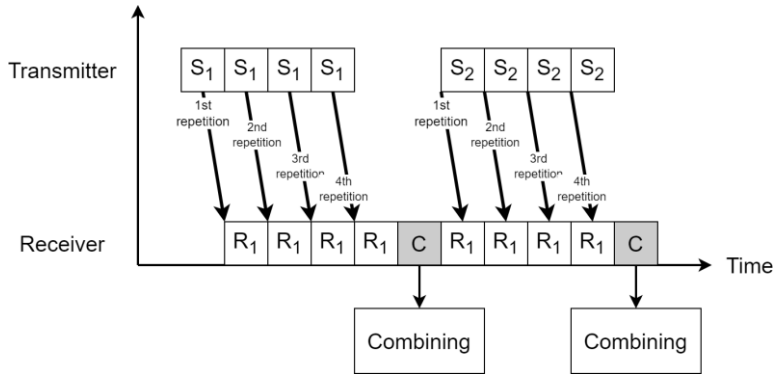


Figure 2.8: A repetitive transmission schema with the spreading factor of 4.

As is mentioned in the explanation of space diversity and repetitive transmission, multiple received signals need to be combined to have the final signal. For the diversity combining techniques, detailed explanations are given in the following chapters.

# 3. SPARSE CODE MULTIPLE ACCESS WITH TIME-SPREADING AND REPETITIVE TRANSMISSION (SCMA-TSRT)

In this chapter, the basics of SCMA are introduced, and detailed information is given as the system model.

Firstly, the key features of SCMA, such as sparse codebook usage, non-orthogonal communication, and spectral efficiency, are discussed, and the mathematical model is introduced. Later, the proposed system model is given, and the mathematical analysis of the proposed model's upper bound is shown. Finally, the computer simulations to evaluate the performance of the proposed model are given.

Through this chapter, the aim is to give a comprehensive understanding of SCMA and demonstrate the superiority of the proposed model to the traditional model.

## 3.1 System Model

In this section, the essential principles of SCMA are introduced, and the proposed model is given.

### 3.1.1 Sparse Code Multiple Access

In the traditional SCMA systems, each codebook is assumed to consist of $J$ $K$-dimensional codewords. $J$ represents the number of users. Here $K$ denotes the number of sub-carriers. The number of non-zero elements in each codeword is denoted by $N$. Accordingly, $J > K$ indicates overloading, and $N < K$ indicates sparseness. A representation of the basic SCMA system is given in Figure 3.1.

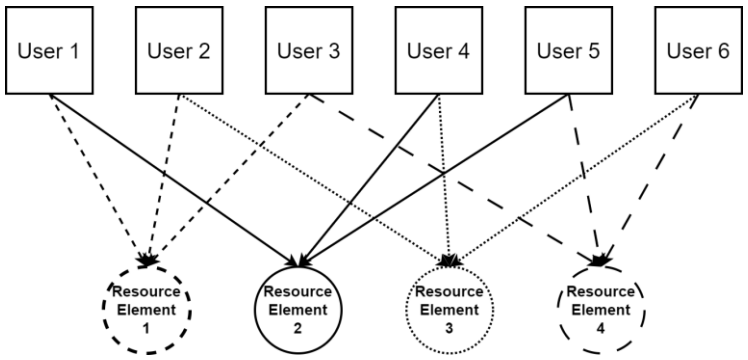


Figure 3.1: Traditional SCMA model with users and frequency resources.

The factor graph matrix **F** is a matrix with K rows and **J** columns and determines the sub-carrier relationship of the users. The commonly used matrix in the literature is given in (3.1) for **J** = 6 and K = 4 [28].

$$\mathbf{F} = \begin{bmatrix} 1 & 1 & 1 & 0 & 0 & 0 \\ 1 & 0 & 0 & 1 & 1 & 0 \\ 0 & 1 & 0 & 1 & 0 & 1 \\ 0 & 0 & 1 & 0 & 1 & 1 \end{bmatrix} \tag{3.1}$$

According to (3.1), each user uses 2 sub-carriers, which is represented as $d_v = 2$, and each sub-carrier is used by 3 users, which is represented as $d_f = 3$.

To analyze the system, firstly, the transmitter and receiver of SCMA are defined. For a single transmission time, the encoder creates a superimposed signal for each sub-carrier. The transmitted data bits **d** for the transmission block b is shown as:

$$\mathbf{d}[b] = [\mathbf{d}_1[b], \mathbf{d}_2[b], ..., \mathbf{d}_j[b]]. \tag{3.2}$$

These data bits are encoded with SCMA encoder. Therefore, for the first step, these

bits are converted to symbols m and shown as:

$$[\mathbf{d}_1[b], \mathbf{d}_2[b], ..., \mathbf{d}_j[b]] \rightarrow [m^{(1)}[b], m^{(2)}[b], ..., m^{(j)}[b]]. \quad (3.3)$$

After symbol conversion, modulation and mapping take place and the end values are shown as:

$$s_j[b] = V_j C_j e^{(M)}_{m^{(j)}[b]}, \quad (3.4)$$

where $M$ is the modulation order, $V_j$ is the mapping matrix per user to sub-carrier and $C_j$ is the constellation matrix per user. $e^{(M)}_{m^{(j)}[b]}$ denotes that $m^{(j)}[b]$-th standart unit vector with dimension $M$ where $m^{(j)}[b] \in Z_M$ for the given data block.

Before the operations of inverse fast Fourier transform, cyclic prefix addition, and parallel-to-serial transformation all of the symbols are summed up and shown as:

$$s[b] = \sum_{j=1}^{J} s_j[b]. \quad (3.5)$$

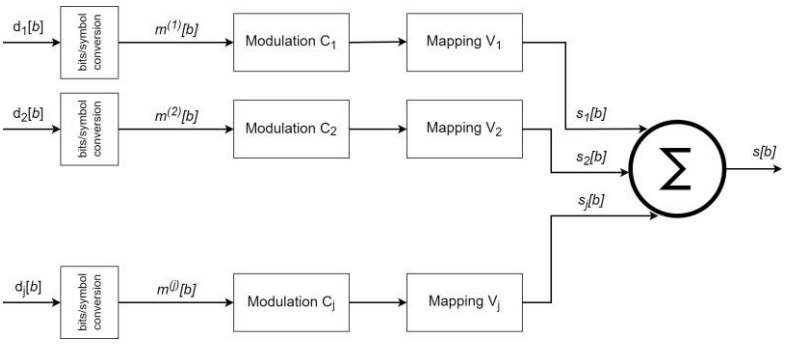


Figure 3.2: Transmitter Block Diagram for SCMA Downlink Systems.

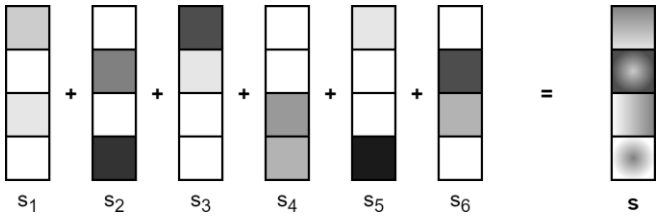


Figure 3.3: Combined signals of 6 users at the transmitter.

The graphical representation of the transmitter block diagram for the given system model of SCMA is shown in Figure 3.2. Also, the superimposed codewords at the transmission are represented in Figure 3.3.

Once the transmission occurs, the received signal at the receiver, after the serial-to-parallel transformation, cyclic prefix removal, and fast Fourier transform, is shown as r[b]. Later the estimated signal for the user j is shown as:

$$\hat{m}^{(j)}[b] = f^{j}_{MP\,A/ML}(r[b]), \tag{3.6}$$

where $f^{j}_{MP\,A/ML}(r[b])$ is a non-linear function, which gives the result of the MPA or maximum likelihood (ML) detection function for the estimated symbol of the user j, given that the received signal is r[b]. A high-level representation of the receiver block diagram for SCMA downlink systems is given in Figure 3.4.

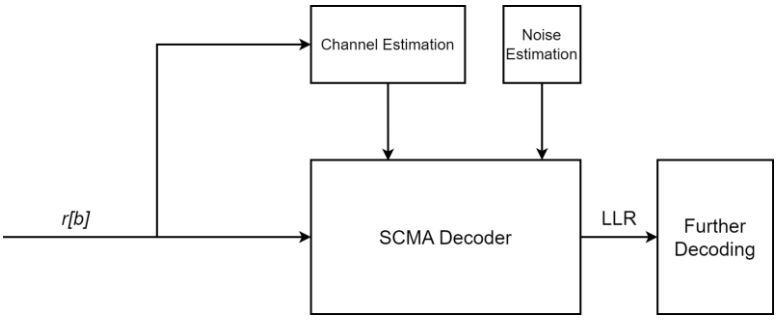


Figure 3.4: Receiver Block Diagram for SCMA Downlink Systems.

At the receiver, the SCMA decoder commonly has two different alternatives to decode and detect the received signals [29].

The first and less frequently used one is the ML detection technique. ML detection problem is NP-hard [30]. This means that there are no existing algorithms with polynomial complexity for its solution. The ML detector aims to obtain an estimation of the message for the given channel conditions and the received signal. Assume the received signal is represented as $r$ and the detected symbol is shown as $\hat{m}$. Then, the detection of the symbol of $j-$ th user for ML is given as

$$\hat{m}^{(j)} = \arg \max_{m \in Z_M} \quad \Pr\{m|r\}, \qquad (3.7)$$

where $M$ here represents the number of codewords per user. A more detailed explanation of ML is given in [31]. The graphical representation of the ML and decision rule is given in Figure 3.5.

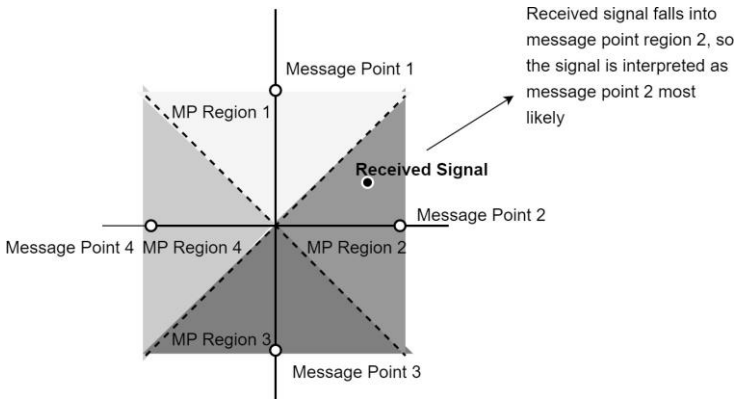


Figure 3.5: Graphical representation of maximum likelihood decision rule.

On the other hand, MPA is the most commonly used technique for SCMA decoding systems. It is a technique that has 3-step procedure and iteratively updates the information at the function nodes (FNs) and variable nodes (VNs) through the factor graph. MPA follows three steps to decode the message. Diagram representation of MPA is shown in Figure 3.6.

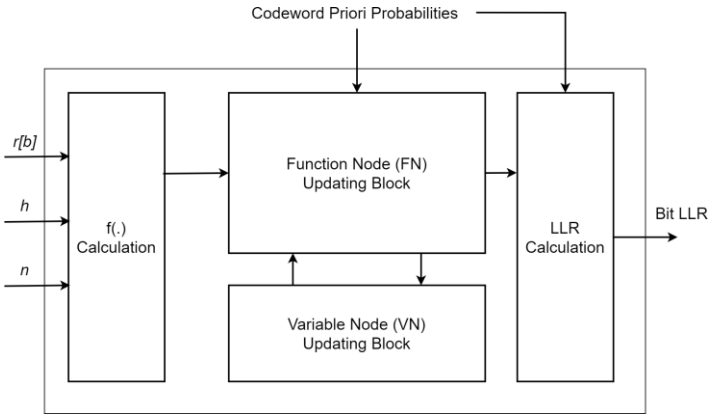


Figure 3.6: Diagram representation of the message passing algorithm.

Firstly, the initial calculations are done for the conditional probabilities. Each variable node (user) is assigned with an a priori probability of $Ap_j = 1/M$, and each

function node (sub-carrier) has the variables of the received signal y, the channel matrix **H** and the noise N. For each function node, the following function is calculated

$$f_n(y_n, m_1, m_2, m_3, N_{0,n}, \mathbf{H^n}) = \frac{-1}{N_{0,n}} \| y^n - \left( h_{n,1} C_{1,n}(m_1) + h_{n,2} C_{2,n}(m_2) + h_{n,3} C_{3,n}(m_3) \right) \|^2, \tag{3.8}$$

where $m_k$ is the codeword selected by layer k, C is the constellation symbol of VN. The initial step is given in Figure 3.7.

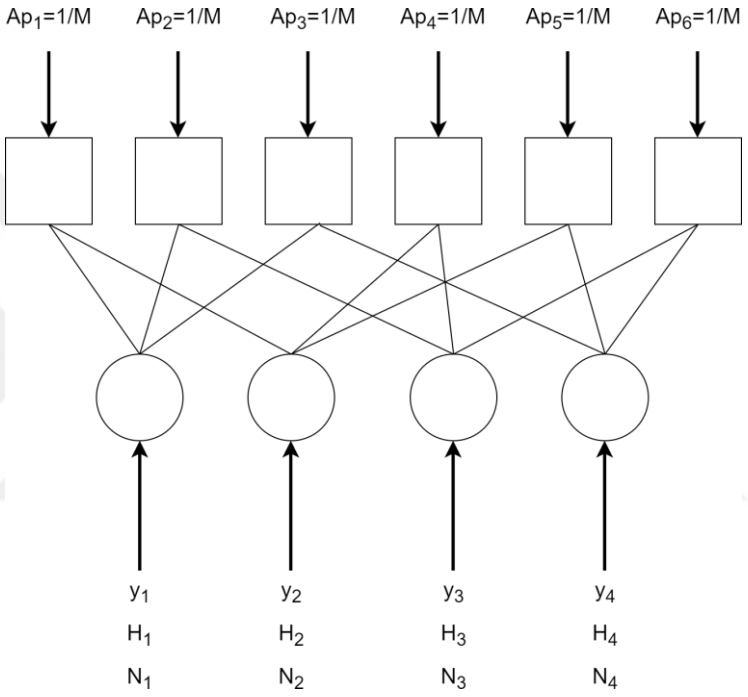


Figure 3.7: Initial calculation of the conditional probabilities.

For the Gaussian noise case, the function shown in (3.8) becomes

$$\Phi_n(y_n, m_1, m_2, m_3, N_{0,n}, \mathbf{H_n}) = e^{f_n(y_n, m_1, m_2, m_3, N_{0,n}, H_n)}, \tag{3.9}$$

and the equally set a priori possibilities are shown as

$$I^{init}_{v_1 \to g}(m_1) = I^{init}_{v_2 \to g}(m_2) = I^{init}_{v_3 \to g}(m_3) = \frac{1}{M}. \tag{3.10}$$

In the second step, the messages are passed along edges iteratively. Firstly, FN is passing messages to its neighboring VNs. As it is shown in Figure 3.8, the FN

node, g, passes the updates obtained from extrinsic information of $v_2$ and $v_3$ to its neighboring FN $v_1$. The passed message contains the estimated signal at g given all the possibilities of $v_1$.

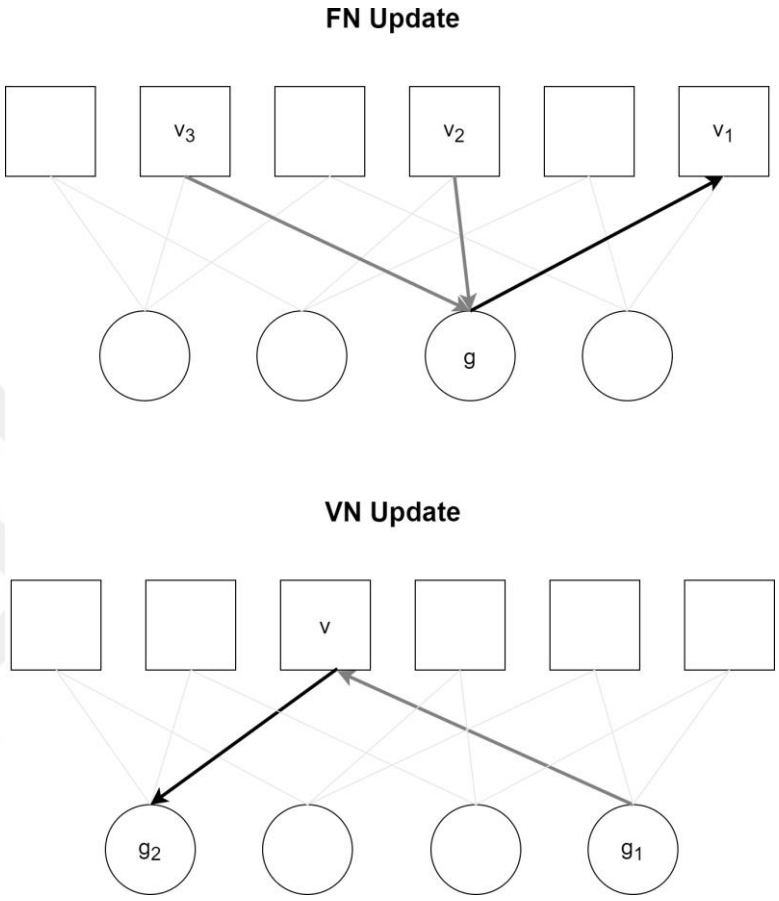


Figure 3.8: Edge updates in the message passing algorithm.

The possibilities are updated as follows

$$I_{g\to v_1}(m_1) = \sum_{m_2=1}^{M}\sum_{m_3=1}^{M} \Phi_n(y_n, m_1, m_2, m_3, N_{0,n}, H_n)\left(I_{v_2\to g}(m_2) I_{v_3\to g}(m_3)\right), \quad (3.11)$$

$$I_{g\to v_2}(m_1) = \sum_{m_1=1}^{M}\sum_{m_3=1}^{M} \Phi_n(y_n, m_1, m_2, m_3, N_{0,n}, H_n)\left(I_{v_1\to g}(m_1) I_{v_3\to g}(m_3)\right), \quad (3.12)$$

$$I_{g\to v_3}(m_3) = \sum_{m_1=1}^{M}\sum_{m_2=1}^{M} \Phi_n(y_n, m_1, m_2, m_3, N_{0,n}, H_n)\left(I_{v_1\to g}(m_1) I_{v_2\to g}(m_2)\right). \quad (3.13)$$

Similar to FN node update, VN node update is also done. The procedure is also shown in Figure 3.8. The updated VN node possibilities are given as

$$I_{v\to g_1}(m) = \text{normalize}\left(Ap_v(m) I_{g_2\to v}(m)\right), \tag{3.14}$$

$$I_{v\to g_2}(m) = \text{normalize}\left(Ap_v(m) I_{g_1\to v}(m)\right). \tag{3.15}$$

In the final step, the log-likelihood ratio (LLR) outputs are obtained after $N_{iter}$ iterations. Graphical representation of the last step is given in Figure 3.9.

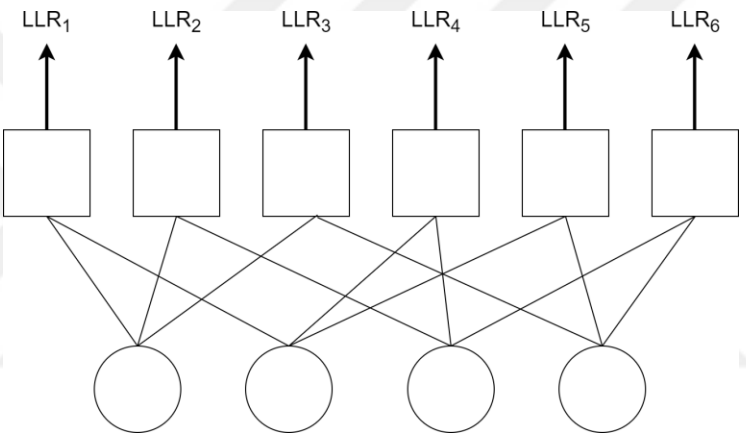


Figure 3.9: Log-likelihood ratio output for the variable nodes.

The guess at VN node v for codeword m is a chain product of all guesses from all its neighboring FN nodes and a priori probability which is given as

$$Q_v(m) = Ap_v(m) I_{g_1\to v}(m) I_{g_2\to v}(m). \tag{3.16}$$

After getting the probability guess of the codeword at each layer, LLR for each coded bit needs to be calculated so that they can serve as the input for the further decoders after MPA. LLR is calculated as

$$LLR_x = \log \frac{(P(b_x = 0))}{P(b_x = 1)}, \tag{3.17}$$

where $b_x$ is the bit value and

$$LLR_x = \log\left(\prod_{m:b_{m,x}=0} Q_v(m)\right) - \log\left(\prod_{m:b_{m,x}=1} Q_v(m)\right). \quad (3.18)$$

In the literature, the SCMA system is usually defined by the parameters of $J = 6$ and $K = 4$; in other words, the system consists of 6 users and 4 sub-carriers [32]. For a fair comparison, the same parameters are employed in this thesis for both analysis and simulations.

### 3.1.2 Integration of Time-Spreading in SCMA

Time-spreading is a commonly used technique for wireless communication systems [33, 34, 35, 36, 37]. However, it has not been widely considered for SCMA systems. The aim of using time spreading is to create a robust system for fast channel fading and also to increase the amount of data transferred in a unit of time. Time-spreading is used in the proposed method to provide spreading codes to multiple users, allowing them to access the same frequency band orthogonally. This increases the overall system's data rate. A graphical representation for a model with two users is given in Figure 3.10.

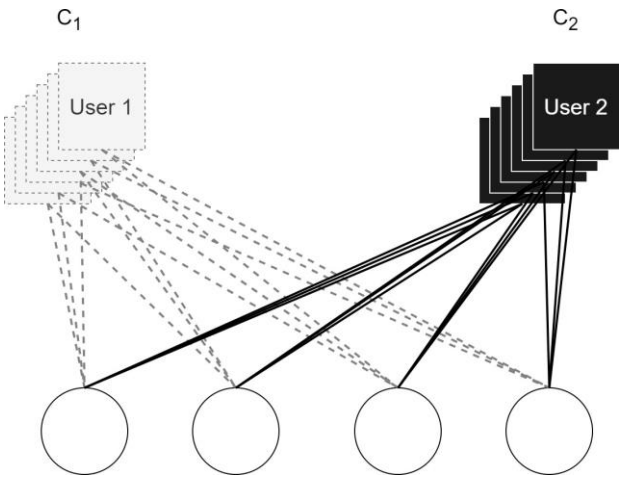


Figure 3.10: SCMA with time-spreading system model with two users.

Orthogonal variable spreading factor (OVSF) codes are used for spreading sequences. Since these codes are minimally cross-correlated with each other, SCMA users can transmit signals without significant inter-user interference [38].

To verify the root of the approach, the SCMA model is first tested with a single user. This way, all of the resources are given to a single user, and sub-carriers are assumed so that no inter-frequency interference exists. To improve the test, a second user is added, and the resources are evenly shared. The results are given in Figure 3.11.

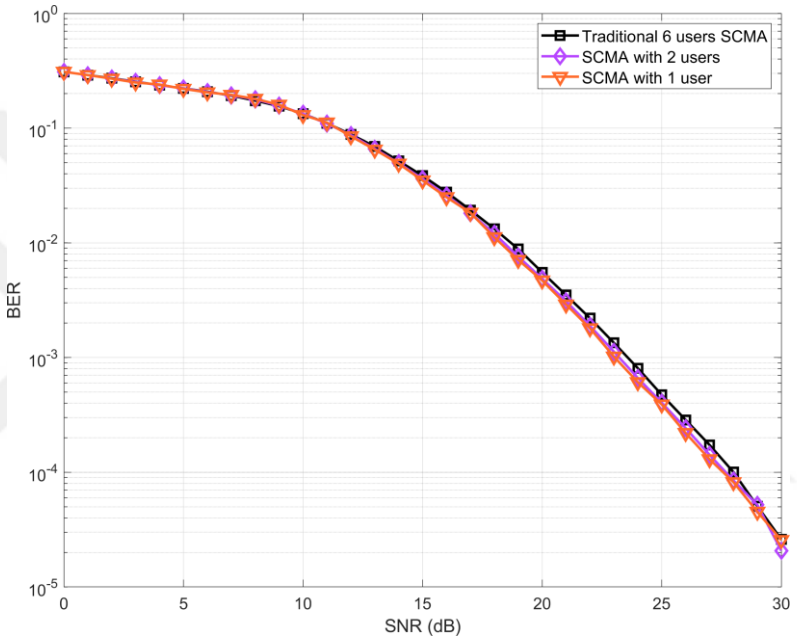


Figure 3.11: Scenario: Traditional SCMA versus the single user or two users use all resources parallel.

It is shown in the figure that SCMA system provides similar results with one user, two users or in a traditional way, six users.

To utilize these users orthogonally, time-spreading is implemented. The transmitted symbol for the given time slot is given as:

$$s_{j,t}[b] = \sqrt{\frac{1}{P}} \times (c_{j,t}[b] \times s_j[b]), \tag{3.19}$$

where $P$ is the average transmit power, $c_{j,t}[b]$ is the time-chip from the time spreading

code for the transmission block b and time slot t. Therefore (4) changes as follows:

$$s_t[b] = \sum_{j=1}^{J} s_{j,t}[b]. \tag{3.20}$$

.

At the receiver, the new received signal is denoted as:

$$r'[b] = \sum_{t=1}^{T} \sum_{j=1}^{J} r_t[b] \times c_{j,t}[b] \tag{3.21}$$

.

The estimated symbol for the user j is given as:

$$\hat{m}'^{(j)}[b] = f_{MPA}(r'[b]). \tag{3.22}$$

The block diagram of the model is presented in Figure 3.12.

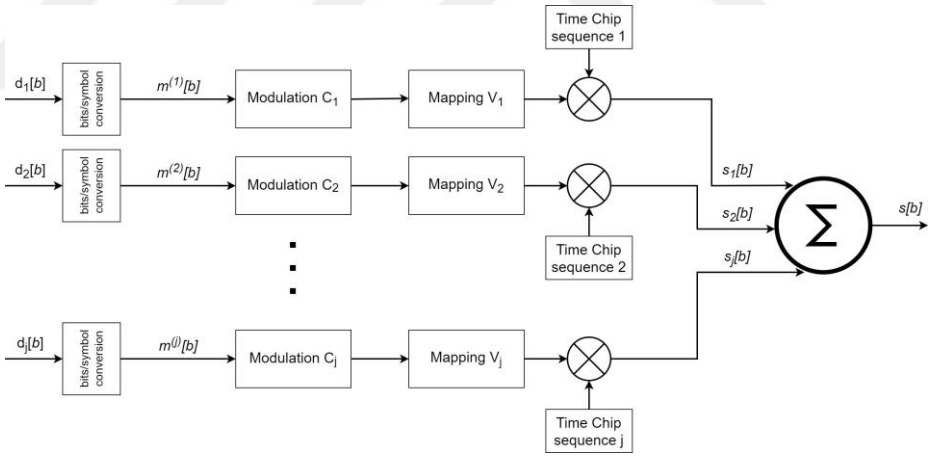


Figure 3.12: Block diagram of the transmitter for downlink system of SCMA with time-spreading.

For validation, the following scenarios are considered

1. One user uses all resources with a spreading factor of 2, 4, and 8
2. Two users use resources with a spreading factor of 2, 4, and 8

3. Comparison of results for different number of users for spreading factor of 8

Figure 3.13 shows the result for a single user using all resources with a spreading factor of 2. This means the user's signal is spread in the time domain twice.

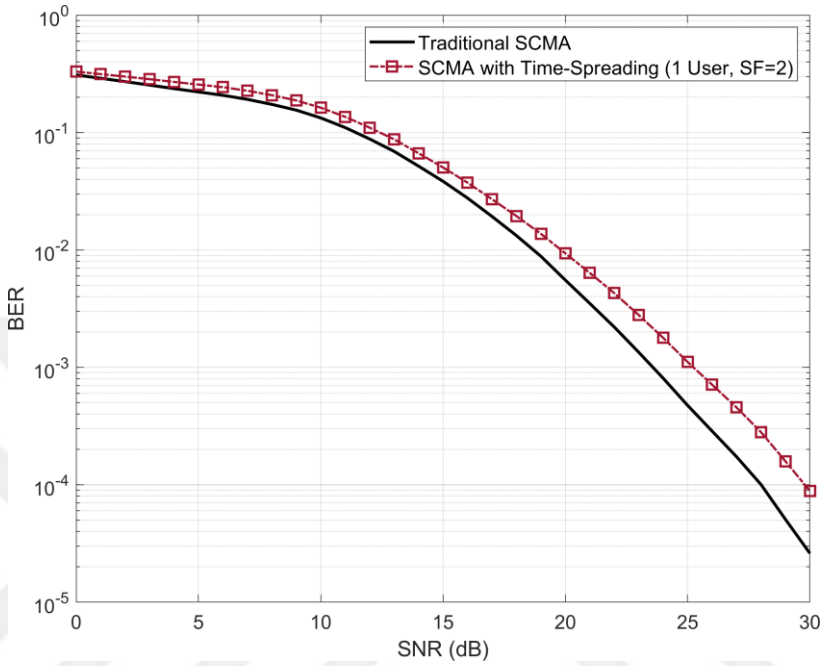


Figure 3.13: Traditional SCMA versus the single user with time-spreading (spreading factor is 2).

It is shown in the figure that time-spreading with a factor of 2 causes a performance loss of around 1.5 dB. To further test the model, results are presented in Figures 3.14 and 3.15 for spreading factors of 4 and 8, respectively.

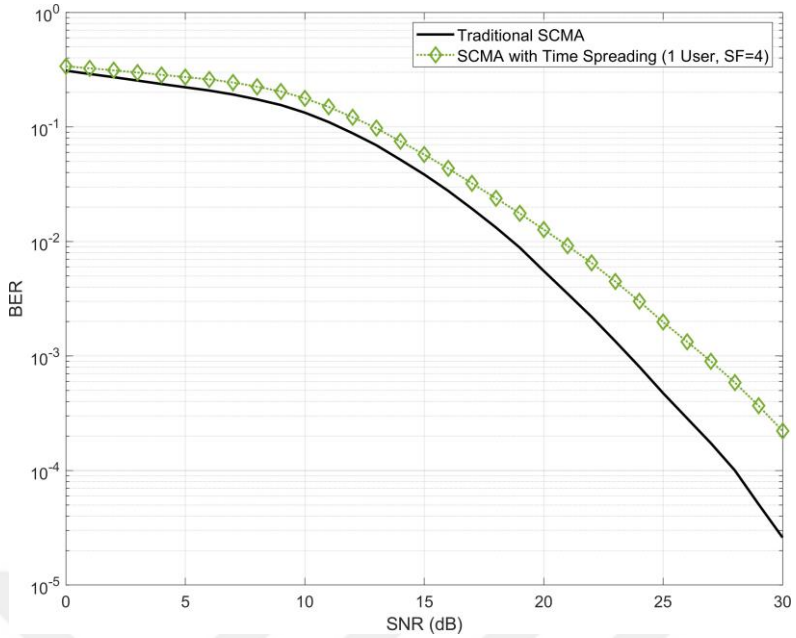


Figure 3.14: Traditional SCMA versus the single user with time-spreading (spreading factor is 4).

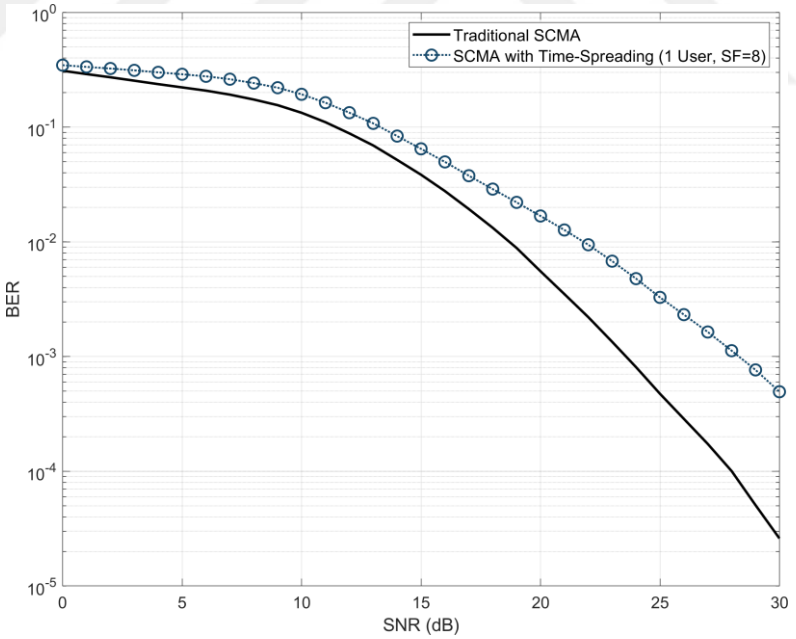


Figure 3.15: Traditional SCMA versus the single user with time-spreading (spreading factor is 8).

Figures show that the increase in the spreading factor increases the loss of perfor-

mance in terms of bit-error. Time-spreading is assumed to increase data rates, which can improve overall system efficiency. While it may lead to a higher error rate in certain scenarios, the increased throughput can help offset any performance drops.

For the second part of the validation simulations, the number of users is increased to two. In Figure 3.16, the comparison of the results given for traditional SCMA, a single user, and two users with the spreading factor of 2.

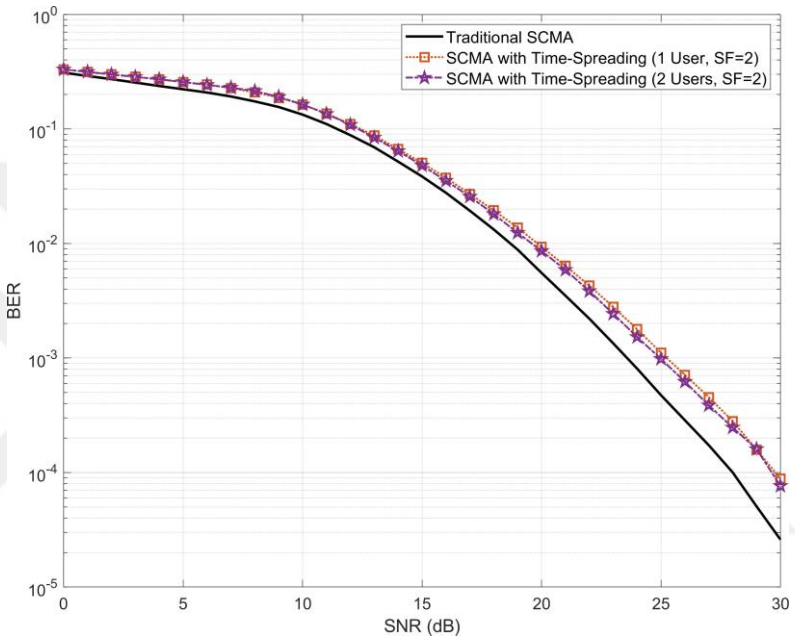


Figure 3.16: Traditional SCMA versus the single user with time-spreading and 2 users with time-spreading (spreading factor is 2).

The figure shows that the number of users in the time-spreading scenario does not affect the bit-error rate performance if the resources are shared equally.

Further results are given for the spreading factor of 4 and the spreading factor of 8 in Figure 3.17 and in Figure 3.18.

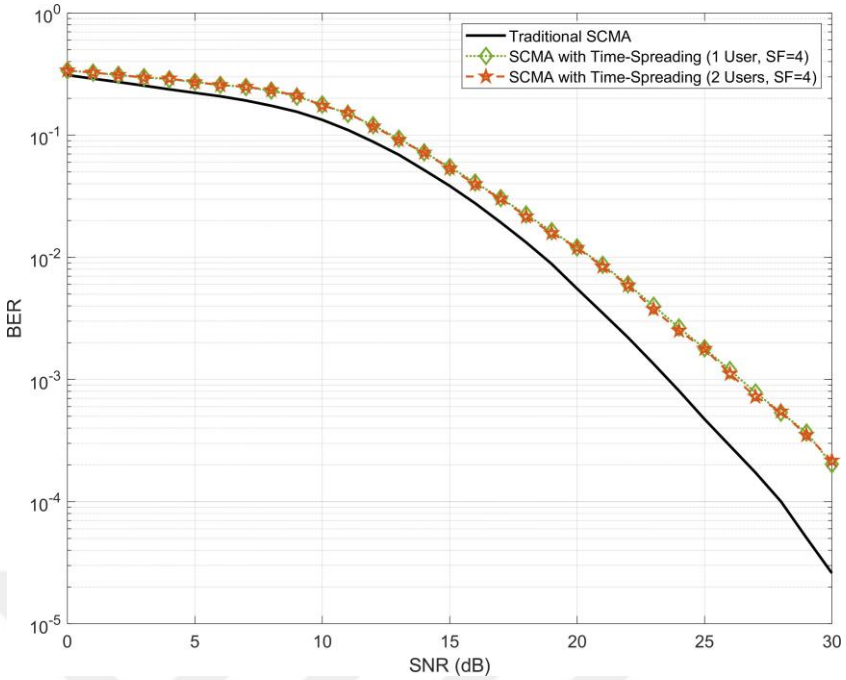


Figure 3.17: Traditional SCMA versus the single user with time-spreading and 2 users with time-spreading (spreading factor is 4).

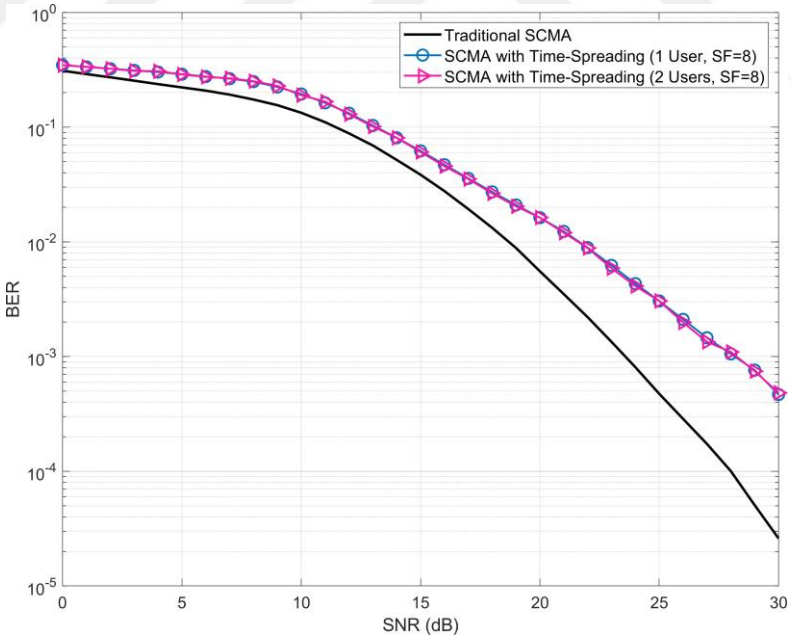


Figure 3.18: Traditional SCMA versus the single user with time-spreading and 2 users with time-spreading (spreading factor is 8).

The results show that the performance results for the spreading factors 4 and 8,

similar to the spreading factor 2, do not make a meaningful difference between the number of users 1 or 2.

As a last validation simulation, keeping the spreading factor constant at 8, the number of users is changed. The result is provided in Figure 3.19. It is shown that the number of users does not make any difference as long as the spreading factor is constant and the resources are equally occupied.

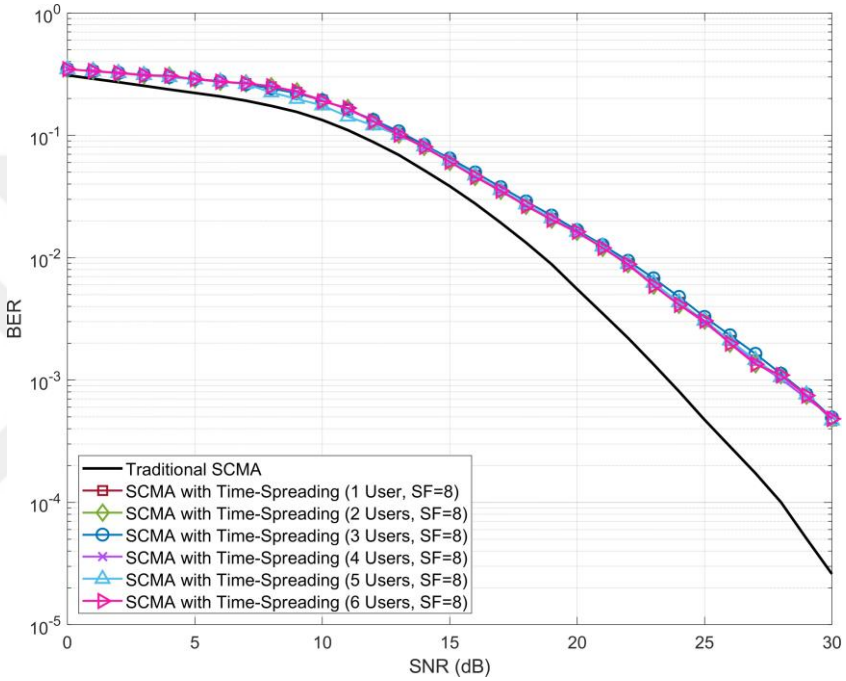


Figure 3.19: SCMA with time-spreading for spreading factor of 8 and various number of users.

In essence, for a single transmission window, users' signal transmissions are divided and spread over time in that transmission window by using time chips. This means that for a single frequency, orthogonal users are accessing the same resource with a dedicated spreading code. This increases the number of data streams by the spreading factor for a single user per time and, therefore, increases the spectral efficiency, which leads to an increased data rate proportional to the spreading factor.

### 3.1.3 Integration of Repetitive Transmission in SCMA

When the energy-per-bit is constant, although the system data rate increases, time spreading would yield lower signal power per time slot, resulting in a lower signal-to-noise ratio (SNR) and deterioration of BER performance. To compensate for the decrease in SNR, repetitive transmissions are incorporated.

Considering repetitive transmissions, the transmitted signal is given by

$$s'_j[b] = [s_{j,1}[b], s_{j,2}[b], ..., s_{j,r-1}[b]], \tag{3.23}$$

where $s'_j$ is the concatenation of $r - 1$ times repeated signal of $s_j$ and $[...]$ denotes the concatenation. Since $s_j$ is repeated $r - 1$ times with the same characteristics, $s_{j,r_1}[b] = s_{j,r_2}[b] = ... = s_{j,r-1}[b]$. The block diagram of the integration of repetitive transmission for the transmitter for downlink systems in SCMA given in Figure 3.20.

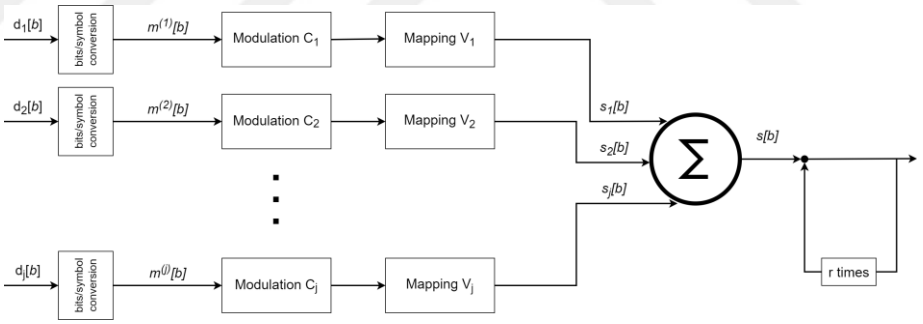


Figure 3.20: Block diagram of the transmitter for downlink system of SCMA with repetitive transmission.

It is assumed that, at the receiver, EGC is used to combine the signals. Therefore, each signal and each channel are considered equal, and the decoding is processed accordingly.

Similar to the earlier section, computer simulations are performed to validate the system model, and a comparison of the results with the traditional SCMA is conducted. The following scenarios considered

1. One user uses all resources with the repetition factor of 2, 4, and 8
2. Two users use resources with the repetition factor of 2, 4, and 8
3. Comparison of results for different numbers of users for the repetition factor of 8

The first scenario gives the results for a single user's scenario. The user uses all resources while employing repetitive transmission with a factor of 2. This means that every signal transmission is performed twice with successive time frames. This has the benefit of reducing the BER up to 1.3 dB, as shown in Figure 3.21. However, due to the double repetition of the signal, throughput is halved.

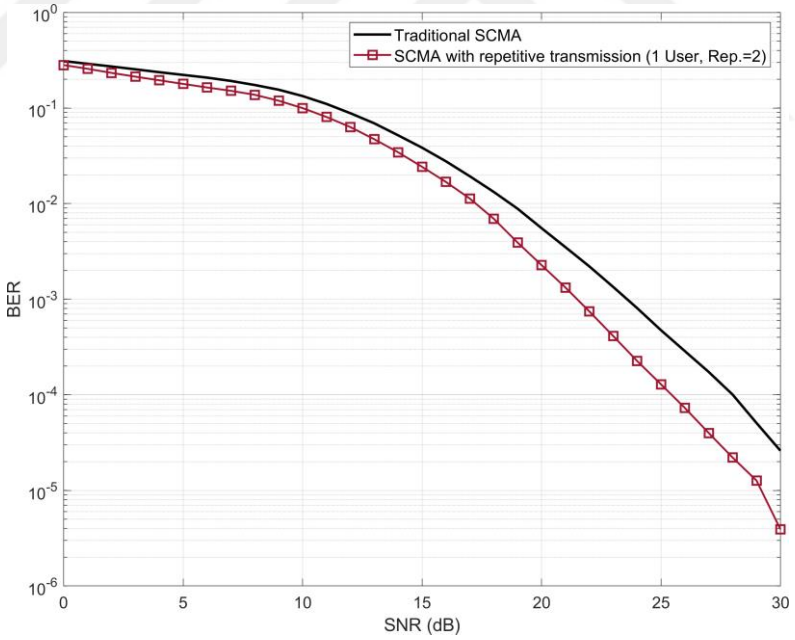


Figure 3.21: SCMA with repetitive transmission for repetition factor of 2.

Further results are presented for the repetition factor of 4 and the repetition factor of 8 in Figure 3.22 and in Figure 3.23.

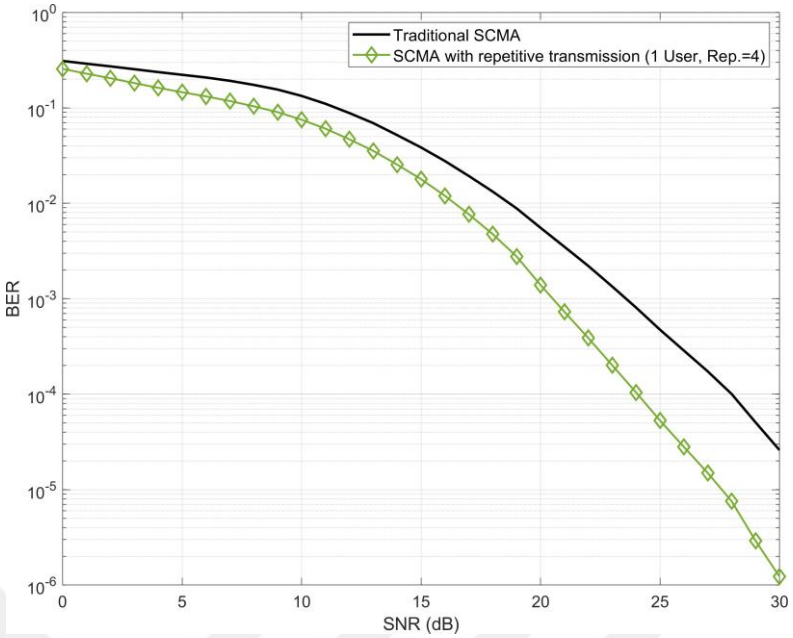


Figure 3.22: SCMA with repetitive transmission for repetition factor of 4.

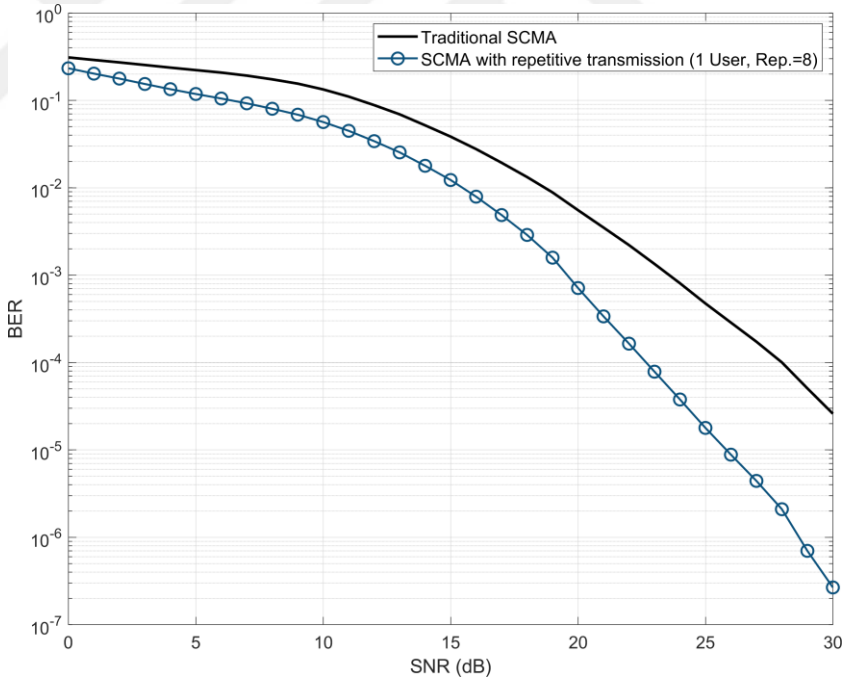


Figure 3.23: SCMA with repetitive transmission for repetition factor of 8.

The figures show that the increased number of repetitions increases the BER performance. However, it should be noted that parallelly, the throughput decreases. While the throughput is 1/8 of the original SCMA, with 8 repetitions, the BER

performance is increased up to 5.5 dB.

For the second scenario, the number of users is set to two. In Figure 3.24, the comparison of the results given for traditional SCMA, a single user, and two users with the repetition factor of 2. The figure shows that the number of users in SCMA with repetitive transmission does not have a significant effect.

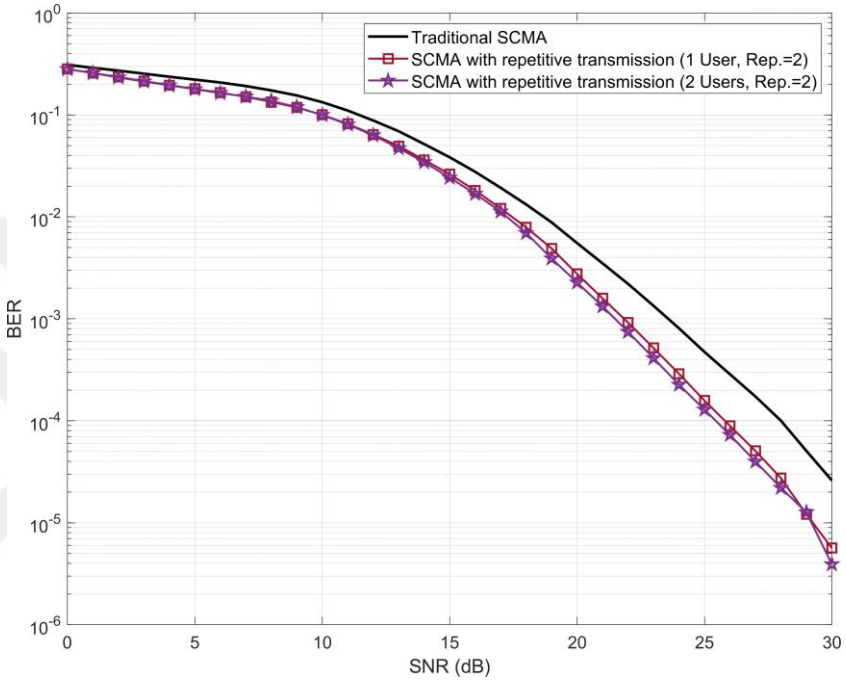


Figure 3.24: Traditional SCMA versus the single user with repetitive transmission and 2 users with repetitive transmission (repetition factor is 2).

Other results are given for the repetition factor of 4 and the repetition factor of 8 in Figure 3.25 and in Figure 3.26.

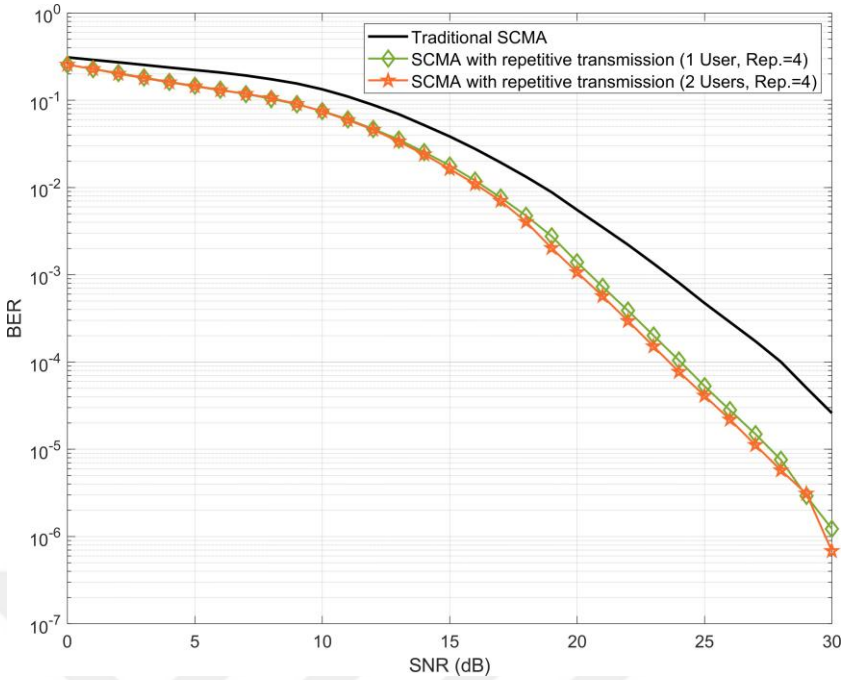


Figure 3.25: Traditional SCMA versus the single user with repetitive transmission and 2 users with repetitive transmission (repetition factor is 4).

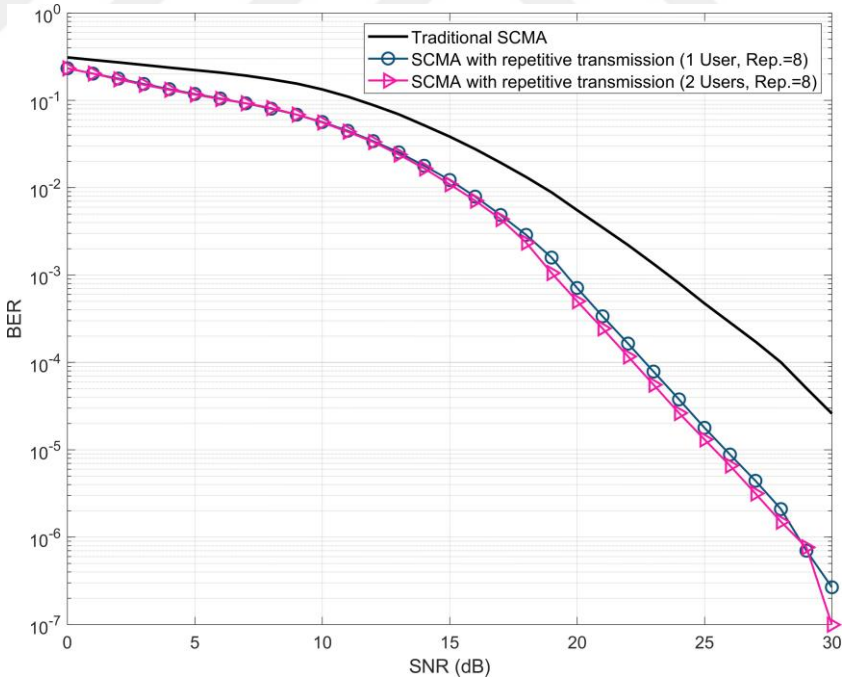


Figure 3.26: Traditional SCMA versus the single user with repetitive transmission and 2 users with repetitive transmission (repetition factor is 8).

The results show that the performance results for the repetition factors 4 and 8,

similar to the repetition factor 2, do not make a significant difference between the number of users 1 or 2.

Lastly, the effect of the number of users is examined by keeping the repetition factor constant. In Figure 3.27, the results given for the repetition factor 8 and the number of users as 1, 2, 3, 4, 5, and 6.

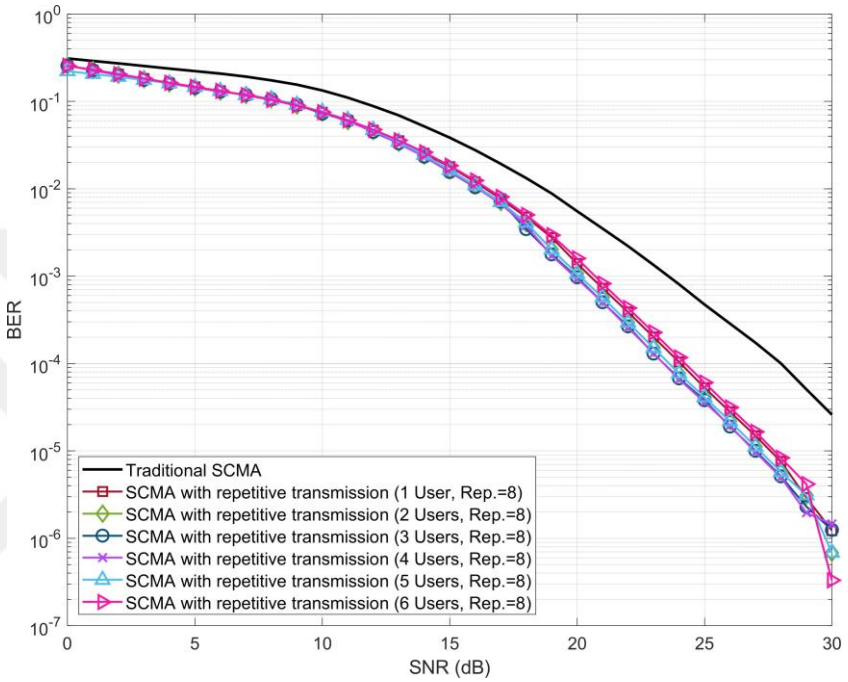

Figure 3.27: SCMA with time-spreading for repetition factor of 8 and various number of users.

It is shown in the figures that the number of users makes little to no difference for SCMA with repetitive transmission. However, the repetitive transmission provides a higher performance of BER when compared to traditional SCMA, while the data rates are dropped due to the repetition.

### 3.1.4 SCMA with Time-Spreading and Repetitive Transmission

When the energy-per-bit is constant, although the system data rate increases, as introduced in the earlier section, time-spreading would cause lower signal power per time slot, resulting in a lower signal-to-noise ratio (SNR) and deterioration of BER

performance. To compensate for the decrease in SNR, the repetitive transmission model is incorporated with the time-spreading model. The graphical representation of the model is shown in Figure 3.28.

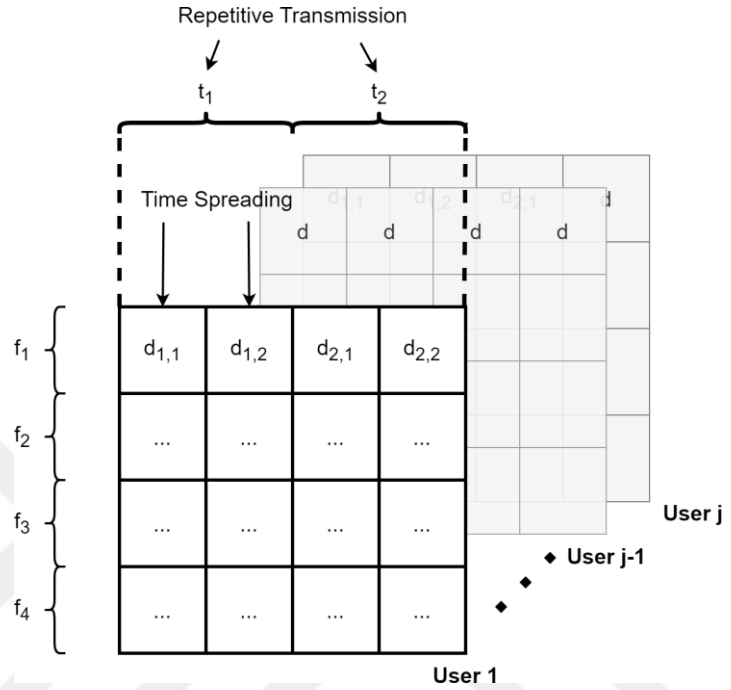


Figure 3.28: Graphical representation of an SCMA-TSRT system with spreading factor of 2 and repetitive transmission factor of 2.

The combined transmitter equation is defined as follows

$$s'_{j,t}[b] = [s_{j,t,1}[b], s_{j,t,2}[b], ..., s_{j,t,r_1}[b]] \tag{3.24}$$

where $s'_{j,t}[b]$ is the concatenation of $r - 1$ times repeated signal of $s_j$. Expanded formula becomes

$$s'_{j,t}[b] = \left[\frac{1}{P} \times (c_{j,t}[b] \times s_j[b]), \frac{1}{P} \times (c_{j,t}[b] \times s_j[b]), ..., \frac{1}{P} \times (c_{j,t}[b] \times s_j[b])\right] \tag{3.25}$$

The block diagram of the transmitter is given in Figure 3.29.

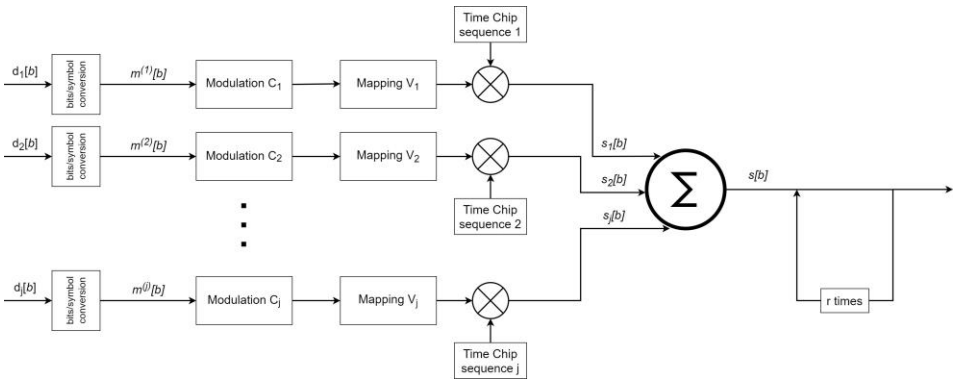


Figure 3.29: Block diagram of the transmitter for downlink system of SCMA with time-spreading and repetitive transmission.

It is assumed that EGC is used at the receiver to combine the signals. The receiver equation becomes

$$r'[b] = \sum_{j=1}^{J} \sum_{i=1}^{r-1} \sum_{t=1}^{T} (r_{t,i}b \times c_{j,t}[b]). \tag{3.26}$$

The block diagram for the receiver is given in Figure 3.30.

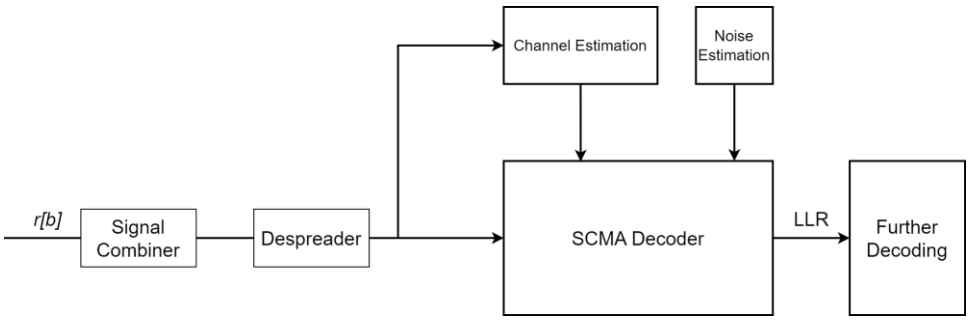


Figure 3.30: Block diagram of the receiver for downlink system of SCMA with time-spreading and repetitive transmission.

## 3.2 Theoretical Upper Bound Analysis

Due to the complexity of detection algorithms such as MPA, it is challenging to derive a closed-form expression for the BER performance of SCMA. In [39], due to the similarity of the error-rate performances of MAP and MPA, the authors suggested comparing MPA-based simulation results and theoretical MAP upper bound results to confirm the simulation results. In [39], the upper bound for the symbol error rate (SER) of the MAP detector is obtained as follows :

$$P_{e,s} \approx P_{e,s}^{MAP} \leq \frac{1}{M^J \cdot J} \mathbf{1}_{M^J}^T (\mathbf{Q} \circ \mathbf{D}_s) \mathbf{1}_{M^J}, \tag{3.27}$$

where the $\mathbf{D}_s \in Z^{M^J \times M^J}$ is the matrix of Hamming distances between every possible multiplexed symbol, $\circ$ is the Hadamard product, and matrix $\mathbf{Q}$ defined as

$$[\mathbf{Q}]_{k,l} = Q\left(\sqrt{\frac{d_{kl}}{2N_0}}\right), \tag{3.28}$$

where $d_{kl}$ is the Euclidean distance between the k-th and l-th possible superimposed codewords. Accordingly, an upper bound for BER, denoted as $P_{e,b}$, can be obtained using (3.27) as

$$P_{e,b} \approx P_{e,b}^{MAP} \leq \frac{1}{M^J \cdot J \log_2 M} \mathbf{1}_{M^J}^T (\mathbf{Q} \circ \mathbf{D}_b) \mathbf{1}_{M^J}, \tag{3.29}$$

where $\mathbf{D}_b \in Z^{M^J \times MJ}$ is the Hamming distance between the bit patterns. The detailed explanations for (3.27), (3.28), and (3.29) can be found in [39]. In Figure 3.31, upper-bound results for two different codebooks [39, 40] and the computer simulation results as a comparison are given.

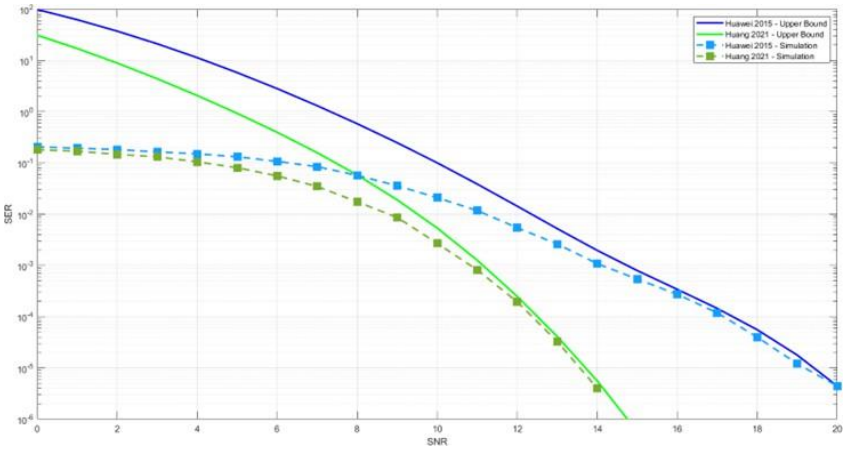


Figure 3.31: SCMA upper bound results for different codebooks and comparison with computer simulation results.

To derive the BER upper bound for the proposed SCMA with time spreading and repetitive transmissions, (3.29) is modified. Consider the following parameters: $L$ is the spreading factor, $R$ is the number of repetitions, and $\gamma$ is the SNR after processing. The number of possible superimposed codewords becomes $J \times L$ and the new set of $d_{kl}$ needs to be computed for $\mathbf{Q}$ for the new possible superimposed codewords. $\mathbf{D}_b$ becomes $\mathbf{D}_{b-s} \in Z^{M^{J\times L}\times M^{J\times L}}$ as an alternative for the distances between each computed possible codeword for spreading factor $L$. In this case, the upper bound of BER for an SCMA system with time-spreading factor $L$ can be computed as:

$$P_{e,b-s} \approx P_{e,b-s}^{MAP} \leq \frac{1}{M^{J\times L} \cdot J \log_2 M} \mathbf{1}_{M^{J\times L}}^{T} (\mathbf{Q} \circ \mathbf{D}_{b-s}) \mathbf{1}_{M^{J\times L}}. \quad (3.30)$$

Adding repetitive transmissions to (3.30) to model the proposed system, $\mathbf{Q}$ needs to be replaced by $\mathbf{Q}'$ as

$$[\mathbf{Q}']_{k,l} = Q\left(\sqrt{\frac{R \cdot d_{kl}}{2N_0}}\right). \quad (3.31)$$

Since EGC is applied, the noise is averaged through $R$ repetitions; therefore, $\gamma$ is $R$ times the SNR without repetitions.

The upper bound for BER obtained using (3.30) is compared to simulation results illustrated in Figure 3.31 for different spreading factors and repetitions under AWGN channel.

It is shown in Figure 3.32 that the time spreading and repetitive transmissions improve BER performance compared to the traditional SCMA system. ”Order” in the figure denotes the number of repetitions and spreading. The figure also illustrates the correlation between the simulation results and the numerical upper-bound results.

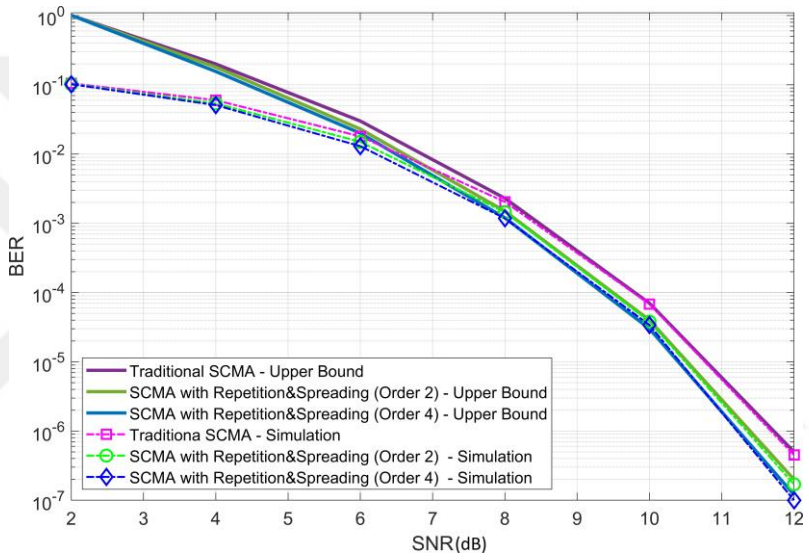


Figure 3.32: SCMA upper bound results for traditional SCMA and proposed model.

## 3.3 Computer Simulation Results For The Proposed Model

In this section, the BER performance of the proposed method is investigated under various scenarios. Some of the results are presented in the earlier sections; however, to ensure the integrity of the topic is maintained, they are mentioned again.

Rayleigh fading channel is considered for all of the simulations. The channel is set to be a frequency-selective channel, and channel coefficients are

$$\mathbf{h} \sim \mathrm{CN}(0, \mathrm{diag}(\sigma^2_{h[0]}, \sigma^2_{h[1]}, \ldots, \sigma^2_{h[Z-1]})), \tag{3.32}$$

where $[\sigma^2_{h[0]}, \sigma^2_{h[1]}, \ldots, \sigma^2_{h[Z-1]}]^T = h_\sigma / \|h_\sigma\|_2$, and $h_\sigma \in \mathbb{R}^Z$ is the vector whose elements are spaced linearly between 0 dB and -48 dB as in [41]. $Z$ here denotes the channel length.

Three scenarios are presented in this section. In each scenario, energy-per-bit is adjusted to allow fair comparison between results. Specifically, in every transmission window, the total energy spent in the system is equal for every scenario. The first scenario illustrates the performance of time-spreading applied to SCMA. In this scenario, with time-spreading, higher data rates are aimed due to the increased spectral efficiency and multiple data streams for each user. This means that the total sum rate is multiplied by the spreading factor in each case. Figure 3.33 shows the results for the first scenario.

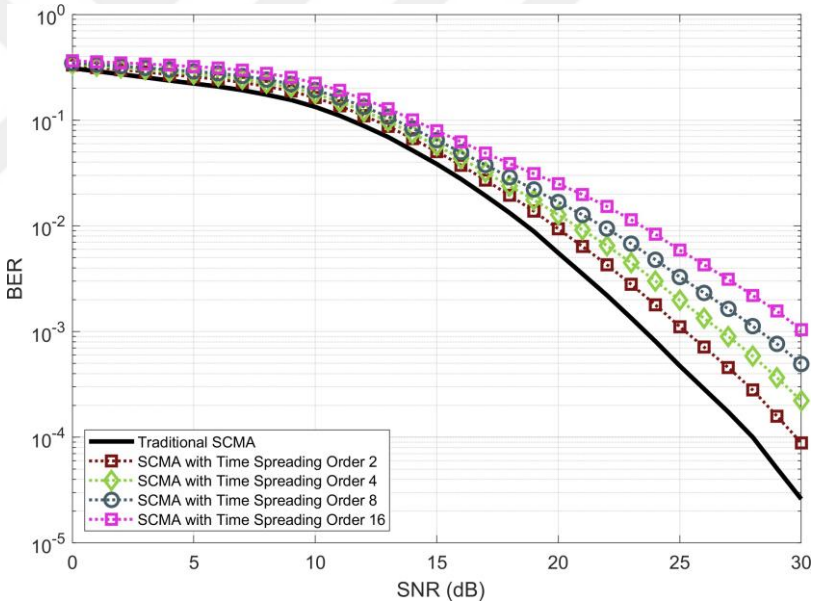


Figure 3.33: BER results under Rayleigh fading channel with different spreading factors for SCMA with time-spreading.

It is shown in Figure 3.33 that with the increased spreading factor, there is a trade-off between the data rate and BER performance. For a spreading factor of 2, there is a loss of around 2.2 dB, and for values of 4, 8, and 16, the loss increases up to 3.5 dB, 5.1 dB, and 6.7 dB, respectively.

The second simulation scenario focuses on the performance of repetitive transmissions applied to SCMA. In this scenario, repetitive transmissions are expected to provide BER performance while decreasing the total sum rate by the number of repetitions. Figure 3.34 gives the results for this scenario.

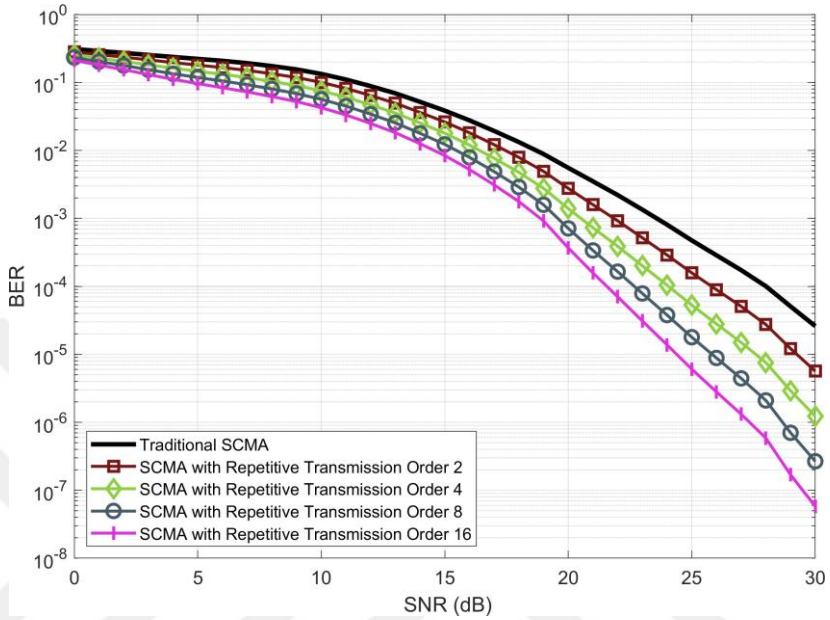


Figure 3.34: BER results under Rayleigh fading channel with different number of transmission repetitions for ”SCMA with repetitive transmission”.

Figure 3.34 shows that the increased number of repetitions increases the BER performance. For a repetition value of 2, around 2 dB gain is observed. On the other hand, for 16 repetitions, the performance gain increases up to 6.5 dB.

Finally, the last scenario reveals the simulation results of the proposed model with both time-spreading and repetitive transmissions under the Rayleigh channel. In Figure 3.35, the results are presented.

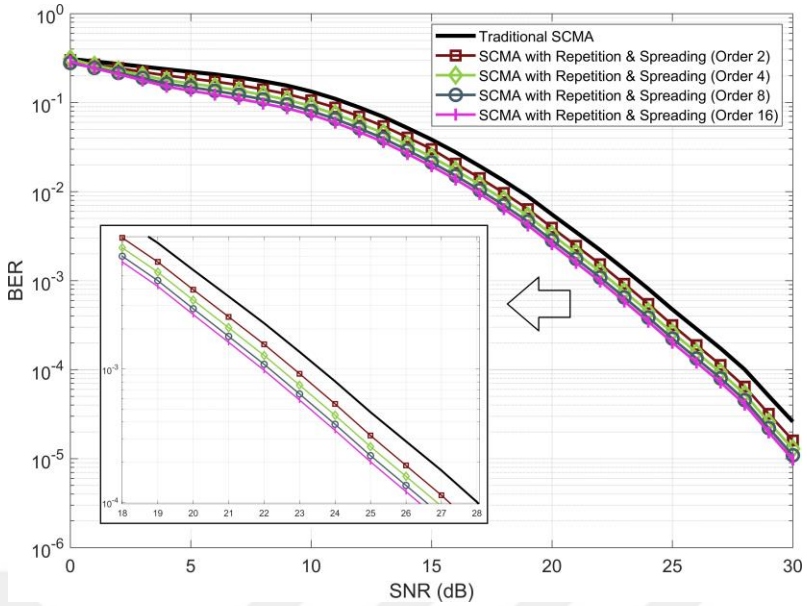


Figure 3.35: BER results under Rayleigh fading channel with different number of variables for the proposed ”SCMA with time-spreading and repetitive transmissions”.

As mentioned in the earlier sections, using time-spreading and repetitive transmissions improves the BER performance of SCMA systems at the same data rate. It is shown in Figure 3.35, under the condition that energy-per-bit is equal in every scenario, for the same overall sum rate, our proposed model improves the BER performance up to 1.6 dB.

## 3.4 Complexity Analysis

In this section, we derive the computational complexity of the proposed method as follows. The complexities of MPA decoding, time-spreading, repetitive transmissions, and EGC are first evaluated separately and then combined to obtain the overall complexity.

The computational complexity of a traditional SCMA system with MPA decoding is derived, in three different steps, in [42]. The number of additions $N^A$, multiplications

$N^M$, and exponentials $N^E$ are given respectively as

$$N^A = (2d_f + 1)M^{d_f}Kd_fN_{iter} + (N - 2)MKd_fN_{iter} + 2MKd_f, \quad (3.33)$$

$$N^M = (d_f + 2)M^{d_f}Kd_f N_{iter} + 4MKd_f, \quad (3.34)$$

$$N^E = M^{d_f}Kd_f N_{iter}, \quad (3.35)$$

where $d_f$ is the VNs per FN, $M$ is the number of codewords per user, $K$ is the number of subcarriers, $N$ is the number of FNs per VN, and $N_{iter}$ is the number of iterations.

For the time-spreading, there are $L$ chips to be evaluated in every transmission period. Therefore, the receiver despreads $L$ chips increasing the number of additions and multiplications as the de-spreading process requires dot products of time chips and the received signal for all subcarriers. In addition, $L - 1$ extra additions are required for each user-subcarrier pair. On the other hand, time-spreading does not introduce additional complexity in terms of exponential operations.

For the repetitive transmissions and EGC, the receiver detects and combines $R$ repeated signals for every transmission period. This increases the complexity in terms of addition operations. All signals received after $R$ repetitions are combined and averaged using EGC. Moreover, since de-spreading is required for each repetition, the additional complexity of the time-spreading is further multiplied by the number of repetitions.

Considering the additional complexity introduced by time-spreading and repetitive transmissions, (3.33) and (3.34) can be reformulated as

$$N^{A} = (2d_f + 1)M^{d_f}Kd_fN_{iter} + (N - 2)MKd_fN_{iter} + 2MKd_f + RNd_f(L - 1) + Nd_f(R - 1), \quad (3.36)$$

$$N^{M} = (d_f + 2)M^{d_f}Kd_fN_{iter} + 4MKd_f + RNd_fL, \quad (3.37)$$

while $N^{E}$ remains the same. The overall complexity comparison is shown in Figure 3.36 for the parameters of $d_f = 3$, $M = 4$, $K = 4$, $N = 2$, $N_{iter} = 3$, $R = 16$ and $L = 16$.

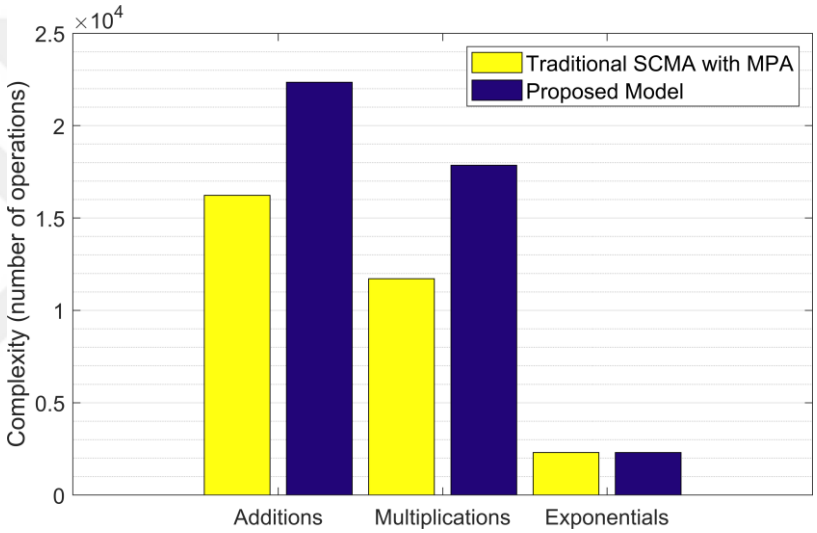


Figure 3.36: Complexity comparison of traditional SCMA and the proposed model.

Further results to compare the proposed model with other state-of-the-art techniques are given in Figure 3.37.

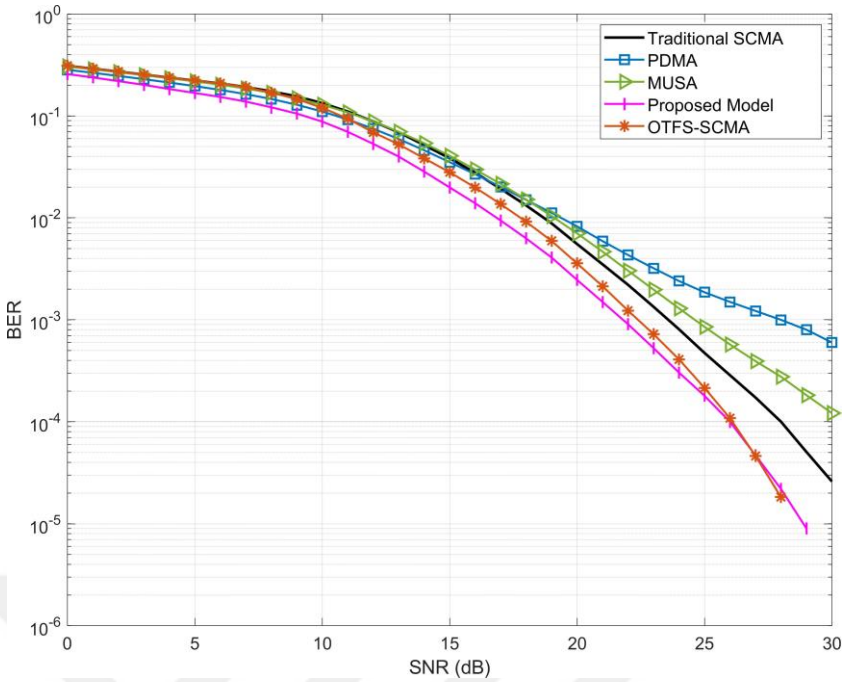


Figure 3.37: Comparison of the proposed model with other state-of-the-art methods.

The results shown in 3.37 that the proposed model is superior in terms of BER performance to MUSA, PDMA, and OTFS-SCMA as well. Although the performance gain is around 0.3 dB against OTFS-SCMA, the proposed model offers lower complexity and higher scalability.

# 4. DIVERSITY COMBINING TECHNIQUES ON SCMA-TSRT

In this chapter, diversity combining techniques are discussed for SCMA-TSRT system. Firstly, traditional techniques are introduced, and adaptations in the SCMA-TSRT system are given with mathematical models. Later, meta-heuristic techniques are introduced to broaden the subject. Lastly, computer simulation results are given.

## 4.1 Traditional Diversity Combining Techniques

Combining techniques are used to transform concatenated signals to provide a valid signal for the transmitter and the receiver to decode, as in multiple antenna systems. Equal Gain Combining (EGC), Maximum Ratio Combining (MRC), and Selection Combining (SC) are the traditional diversity-combining techniques employed in wireless communication systems [43, 44, 45].

EGC combines received signals of equal amplitude using multiple antennas at the receiver and maximizes the total signal strength by adjusting the phase of these signals. This method provides reliable performance in multiple-stream signal transmission.

Assume a system with $N$ transmissions, the received signal denoted as $r_i$ where $i = 1, 2, ..., N$ and shown as

$$r_i[t] = h_i[t]x_i[t] + n_i, \tag{4.1}$$

where $x_i$ is the transmitted signal, $h_i$ is the channel gain and $n_i$ is the noise for the $i-th$ transmission. EGC obtains the combined signals $R$ as follows

$$R_{EGC} = \sum_{i=1}^{N} \frac{h_i^*}{|h_i|} r_i, \tag{4.2}$$

where $h_i^*$ is the complex conjugate of the channel gain $h_i$.

On the other hand, SC selects the best branch based on the highest SNR from the multiple transmission streams. Assume the system same with EGC as $N$ transmissions, received signal $r_i$ where $i = 1, 2, ..., N$, then the combined signal $R$ is shown as

$$R = r_k \quad \text{where} \quad k = \arg\max_i |h_i|. \tag{4.3}$$

Lastly, MRC provides optimal weights to each branch in terms of SNR. The MRC technique takes into account the instantaneous channel conditions and maximizes SNR, therefore maximizing overall performance. MRC combines the signals and obtain $R$ as

$$R = \sum_{i=1}^{N} w_i r_i \tag{4.4}$$

where $w_i$ is calculated as

$$w_i = \frac{h^*_i}{|h_i|^2} \tag{4.5}$$

In SCMA-specific applications, as in [46], considering the complexity at the receiver side, EGC combines the received signal. Therefore, the combined signal can be shown as

$$r_{i,t-EGC}[b] = \frac{\sum_{r=1}^{R} w_i y_{t,r}[i]}{R} \times \sqrt{P_t} \tag{4.6}$$

where $r_{i,t}$ is the received signal at the i-th subcarrier on r-th repetitive transmission and $R$ is the total number of repetition. $w_i$ is the weight assigned based on SNR of each transmission being equal and is equal to 1. After EGC, MPA is used to detect each symbol for each user.

To deploy MRC, the equation changes as

$$r_{i,t-MRC}[b] = \frac{\sum_{r=1}^{R} w_i y_{t,r}[i]}{R} \times \sqrt{P_t} \tag{4.7}$$

where $w_i$ is

$$w_i = \frac{h_r^*[i]}{|h_r[i]|}. \tag{4.8}$$

Here h denotes the channel attenuation coefficient and for selection combining the equation becomes

$$r_{i,t-SC}[b] = \frac{\sum_{r=1}^{R} w_i y_{t,r}[i]}{R} \times \sqrt{P}, \tag{4.9}$$

where $w_i$ is

$$w_i = \begin{cases} 1 & |h_r[i]| = \max\{h_r[i]\}, \forall i \\ 0 & \text{otherwise} \end{cases}.$$

Each technique has its advantages, offering a trade-off between complexity and performance, and is chosen based on the specific requirements and characteristics of the communication system [47].

## 4.2 Metaheuristic Diversity Combining Techniques

Besides conventional diversity combining techniques, new techniques are considered based on evolutionary algorithms. Similar to [48], in addition to conventional techniques, in this paper, genetic algorithm (GA), and imperialist competitive algorithm (ICA) are considered.

Using diversity combining techniques aims to optimize SNR so that BER results improve. For this reason, firstly, SNR is defined as follows in MRC:

$$\gamma_T(\vec{w}) = \frac{1}{\sigma_n^2} \frac{\left|\sum_{i=1}^{R} w_i h_i\right|}{\sum_{i=1}^{R} |w_i|^2}, \tag{4.10}$$

where $\vec{w} = [w_1, w_2, ..., w_R]$ and R is the number of repetition. Evolutionary algorithms are offered to use so that all possible weighting vectors $\vec{w}$ are considered and w's are optimized to maximize the SNR. This way, the need for channel state information estimation is also eliminated.

In the genetic algorithm (GA), a group of chromosomes is initially generated randomly. The fitness function equation (4.10) is used to evaluate the SNR of these chromosomes. Then, a new population is reproduced from the previous one based on the fitness scores (SNR values) of the chromosomes. This process continues until a predefined termination criterion is met [49]. The concept of survival of the fittest/best chromosomes allows for the continuous formation of better populations. The graphical representation of the concept is given in Figure 4.1.

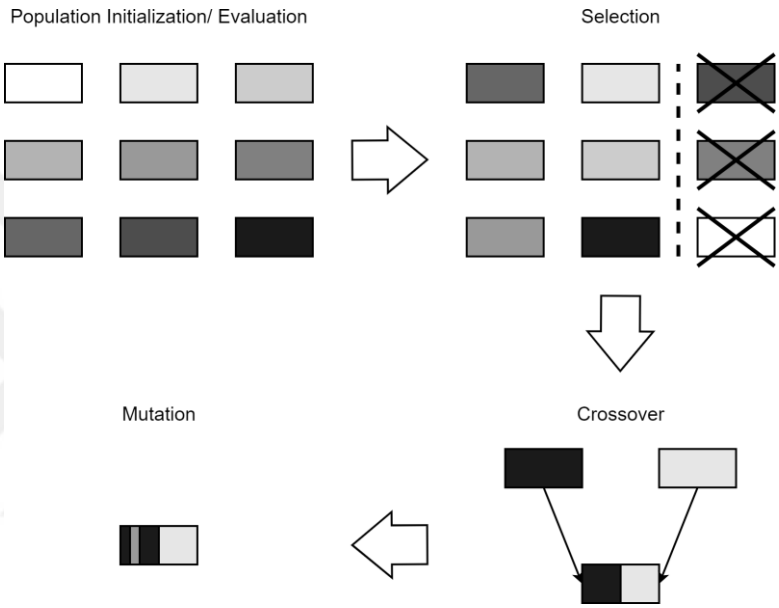


Figure 4.1: Graphical Representation of the Genetic Algorithm.

In genetic algorithm terminology, the process of forming an offspring population from a parent population is called a generation [50]. The number of generations produced is predetermined by the designer or set based on the quality of obtainable solutions. The algorithm is configured to maximize the SNR, and its outline is as follows.

1. Population chromosomes are generated randomly.
2. Each chromosome is decoded into its weighting vector $\vec{w}_j = [w_{j1}, w_{j2}, \ldots, w_{jM}]$, where $w_{ji} \in [0, 1]$ and $i = 1, 2, \ldots, M$ and $j = 1, 2, \ldots, pops$.
3. SNR values are computed for every decoded weighting vectors $\vec{w}_j$ with (4.10)

and rank and identify $\lfloor pops * elite \rfloor$ chromosomes that have maximized SNR. elite is a parameter that determines a fraction of pops, that is, $elite \in [0, 1)$.

4. After large enough generations (iterations at the algorithm), if the output SNR of the system converges to a stable value at each iteration, the procedure is terminated. Otherwise, increase the generation number by one.
5. Reproduce $\lceil pops*(1-elite) \rceil$ new chromosomes and construct new population by concatenating the newly $\lceil pops * (1 - elite) \rceil$ reproduced chromosomes with the best $\lfloor pops * elite \rfloor$ found in Step 3. Jump to Step 2.

Finally, the optimal weighting vector (decoded chromosomes) that leads to the highest stable value of the output SNR can be indicated and used.

For SCMA-TSRT, GA provides a set of weights $\vec{w}_{optimal-GA}$ to combine diverse signals from repetition in the model. The algorithm for GA is given in Algorithm 1.

**Algorithm 1** Genetic-Algorithm Based Diversity Weighting Scheme

**Input:** $N_{par}$, $r_{rate}$, $m_{rate}$, $c_{rate}$

**Output:** $\vec{w}_{optimal-GA}$

1: Generate a random population of $p$ with the population size $p_{size}$ which translates into ($\vec{w}^{*}$) where $w_0^*, w_1^*, ..., w_{p_{size}}^* \in [0, 1]$
2: Compute fitness value (SNR) by using (4.10)
3: Select the highest SNR weight value as parents with the number of $N_{par}$ and then create a new population with a reproduction rate of $r_{rate}$ with mutation rate $m_{rate}$ and crossover rate $c_{rate}$
4: Iterate until the optimal solution is reached for (4.10)
5: Obtain $\vec{w}_{optimal-GA}$

The imperialist competitive algorithm is a subset of optimization algorithms called metaheuristic algorithms. The algorithm is proposed by Atashpaz et. al. in [51]. The motivation of the algorithm is based on the social and political behaviors of countries. In the algorithm, two types of countries are identified as either *a colony* or *an imperialist*, and collectively they form *empires*. The definition of competition

among these empires is the basis of ICA. The aim is to find the optimum points by collapsing weak empires and strengthening the powerful ones by allowing a powerful empire to defeat the other empires. The steps of the modified ICA are given in the Algorithm 2.

**Algorithm 2** Imperialist Competitive Algorithm Based Diversity Weighting Scheme

**Output:** $\vec{w}_{optimal-ICA}$

Initialization: $\vec{w}_0, \vec{w}_1, ..., \vec{w_{p_{size}}}$ where $w_{i,0}, w_{i,1}, ..., w_{i,p_{size}} \in [0, 1]$

Compute $\gamma_T(\vec{w})$ $\forall$ w as in 4.10

$N_{emp}$ of highest SNR $\vec{w} \leftarrow \vec{we_{mp}}$

The rest $\vec{w} \leftarrow \vec{w_{col}}$ where $N_{col} = p_{size} - N_{emp}$

Randomly form $N_{emp}$ of empires with one $\vec{we_{mp}}$ and one or more $\vec{w_{col}}$. The total number of countries in the empire is N.

Compute $P_{emp} = \frac{P_{N}\ \gamma_T(\vec{w_i})}{N}$

**while** $N_{emp} \neq 0$ **do** ▷ Assimilation Process starts

  **while** $j \neq N_{col}$ **do**

    $\vec{w_{new,col_j}} = \vec{w_{old,col_j}} + \vec{x}_j + \vec{r} \cdot \tan(\theta)$

    **if** $\gamma_T(\vec{w_{new,col_j}}) > \gamma_T(\vec{we_{mp}})$ **then**

      $\vec{w_{new,col_j}} \leftarrow \vec{we_{mp}}$

    **end if**

  **end while**

**end while**

**while** $N_{emp} \neq 1$ **do** ▷ Competition between empires starts

  $\min \gamma_T(\vec{w_{col}})$ in empire with $\min P_{emp}$ is provided to empire with $\max P_{emp}$ and Recalculate $P_{emp}$ for all

  $N \leftarrow N - 1$ for the given empire

  **if** $N = 1$ **then**

    $\vec{w_{imp}}$ joins the best empire

    $N \leftarrow 0$ and $N_{emp} \leftarrow N_{emp} - 1$

  **end if**

  **if** $\forall \vec{w} = \vec{w}_{emp}$ & $N_{emp} = 1$ **then**

    $\vec{w}_{optimal-ICA}$ is obtained ▷ If there is only one empire left with the equal-weighted colonies

  **end if**

**end while**

In Algorithm 2, $N_{emp}$ indicates the number of imperialist vectors and empires, and $p_{size}$ indicates the total number of countries. $\vec{w}$, $\vec{w}_{emp}$ and $\vec{w}_{col}$ show the weighting vector, weighting vector for an imperialist and weighting vector for a colony respectively. $\theta$ indicates the assimilation deviation, $P_{emp}$ represents the power of an empire, and $\vec{w}_{optimal-ICA}$ represents the optimal weighting vector solution obtained at the end of the ICA algorithm. A graphical representation of the imperialist competitive algorithm is given in Figure 4.2.

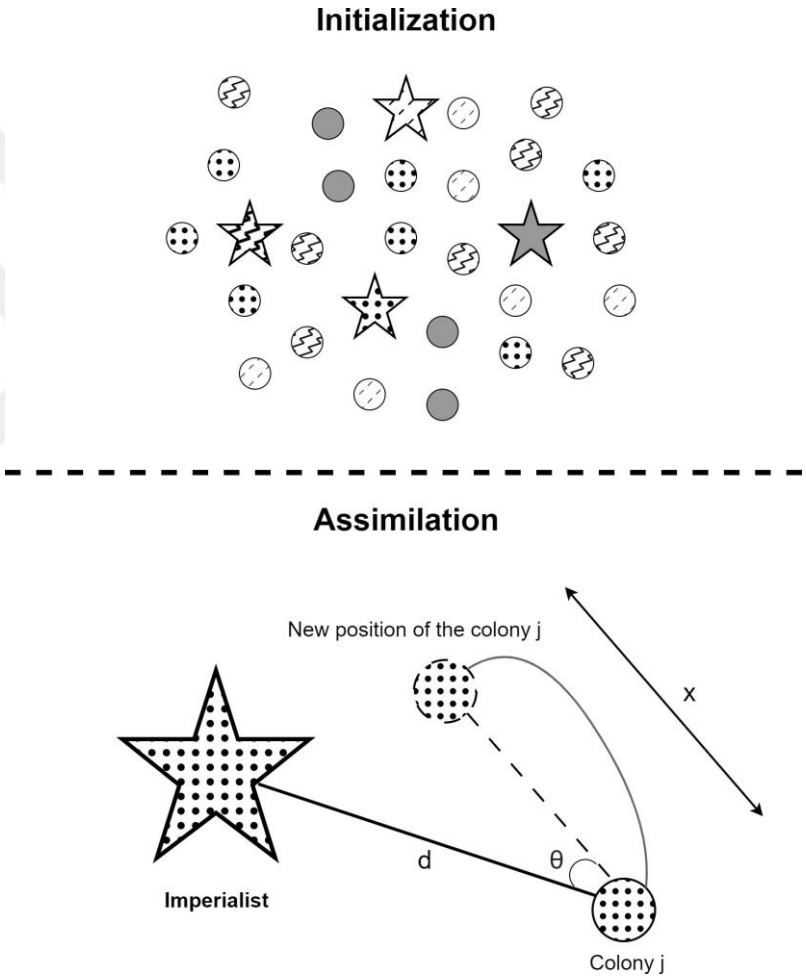


Figure 4.2: Initialization and assimilation steps of Imperialist Competitive Algorithm.

| Parameter Name | Parameter Value |
|---|---|
| Users | 6 |
| Sub-carriers | 4 |
| Transmitted bits per user | $10^8$ |
| Modulation level | 4 |
| Channel model | Rayleigh Fading |
| Codebook | SCMA Huang [39] |
| Spreading factor | 2, 4, 8, 16 |
| Transmission repetition | 2, 4, 8, 16 |
| GA Population size | 50 |
| GA Mutation rate | 3 |
| GA Crossover rate | 0.95 |
| GA Population for reproduction rate | 0.9 |
| ICA Assimilation Coefficient | 1.7 |

Table 4.1: Computer Simulation Parameters

## 4.3 Computer Simulation Results

To analyze the details of the model, Monte-Carlo simulation is employed. The aim is to compare the performances of different diversity techniques mentioned in earlier sections. The average bit energy is assumed to be equal in all scenarios as $E_b = 1$. All simulations were run on MATLAB. The parameters used in the simulations are given in Table 4.1.

Firstly, the normalized average output SNR is given in Figure 4.3. SC, EGC, GA, and ICA are shown in the figure. Alongside, MRC under two different channel estimation conditions, $\rho = 0.5$ and $\rho = 0.8$ are given, where $\rho$ denotes the normalized estimation error correlation coefficient. It is shown that under imperfect channel estimation conditions, both ICA and GA perform better in terms of average output SNR, and the worst performance is obtained when SC is employed. It is worth noting that as the number of diversity elements increases, the performance gain

slope tends to decline. This is because adding more diverse elements may result in marginal returns due to increased complexity and interference. Therefore, finding the optimal number of diversity elements that can provide the maximum performance gain without sacrificing the system's efficiency and complexity is important. In this section, the maximum number of diversity elements is kept at 16 to provide a reasonable complexity for future works to replicate and compare the results.

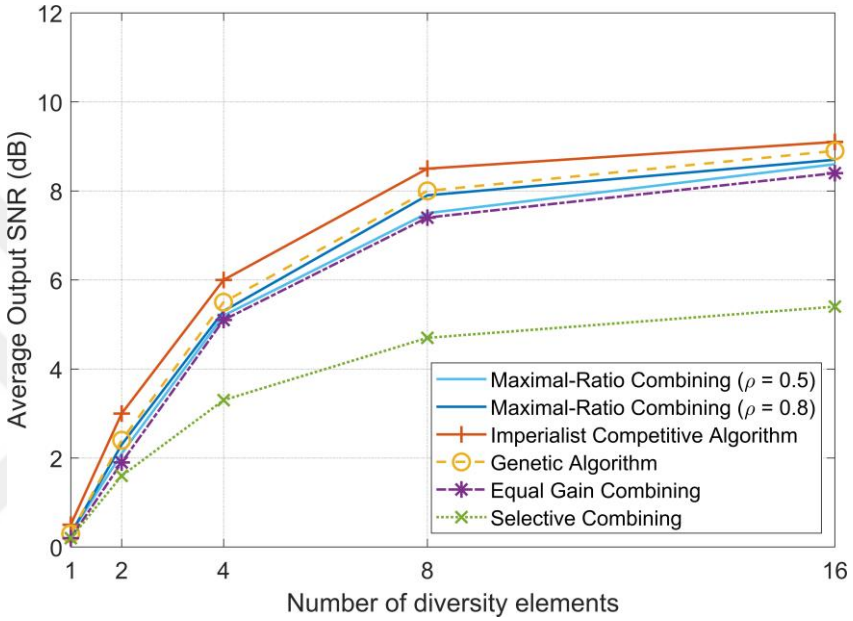


Figure 4.3: Normalized output SNR for different diversity combining techniques.

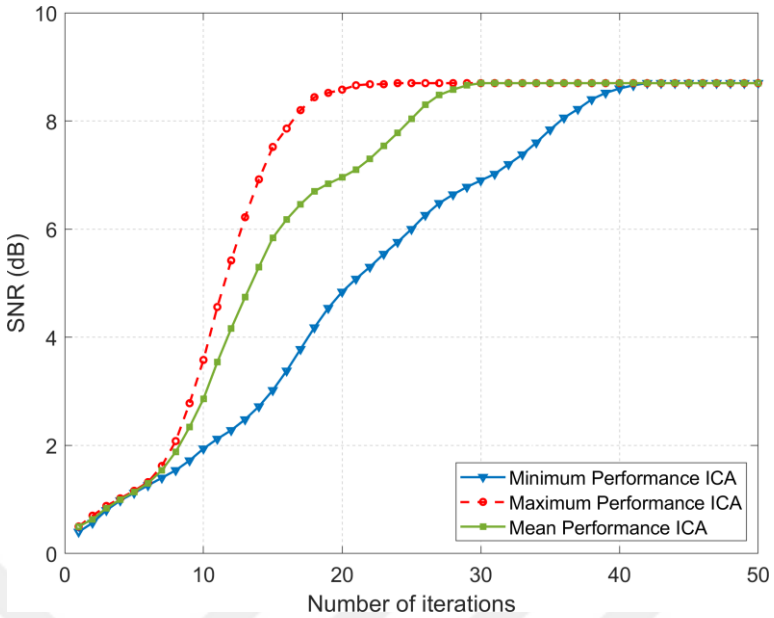


Figure 4.4: Number of iterations required for convergence in ICA for diversity order 16.

It is important to determine the number of iterations required for convergence in ICA since incorporating complex diversity techniques may add unnecessary complexity to the system. In Figure 4.4, the minimum, maximum, and mean performances of ICA in terms of the number of iterations required for convergence are shown. The simulations reveal that the worst-case scenario requires around 40 iterations, while the mean is approximately 27 iterations, and the best-case scenario requires 20 iterations.

Considering the imperfect channel estimation and repetitive transmission in SCMA with time spreading, bit-error-rate results are provided in Figure 4.5 and zoomed version of the figure is provided in Figure 4.6 for diversity order 2.

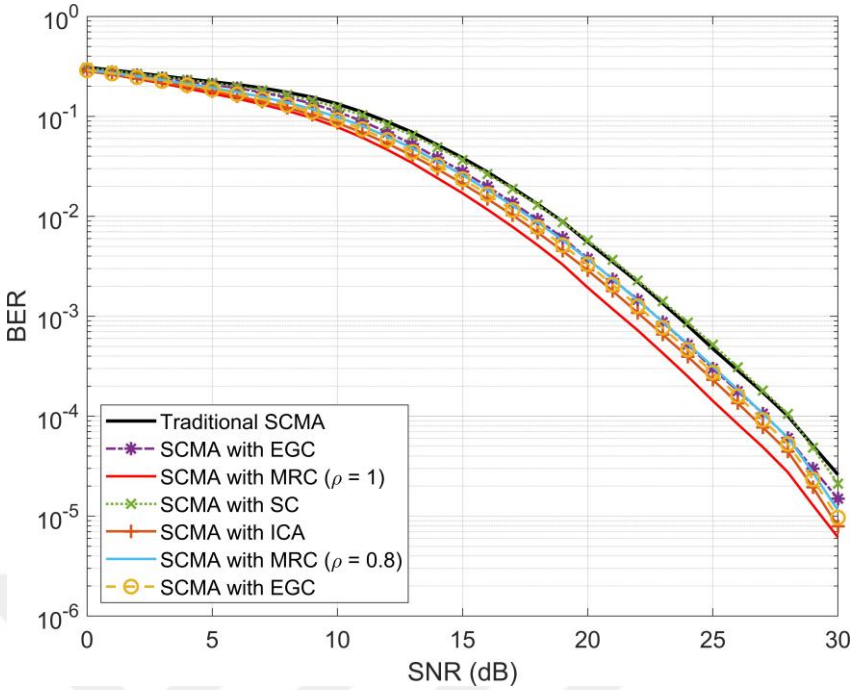


Figure 4.5: Bit-Error Rate Performance Comparison for EGC, MRC, SC, ICA, and GA for diversity order 2.

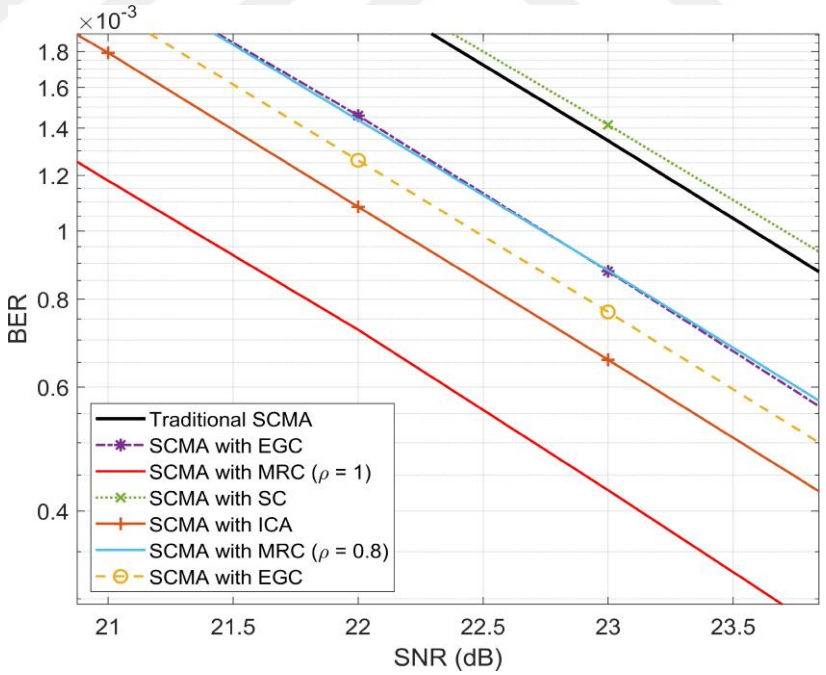


Figure 4.6: Zoomed-in version of Figure 4.5 for BER of $10^{-3}$.

It is shown in Figure 4.5 and Figure 4.6 that SCMA with ICA provides around 1.4 dB gain in terms of bit-error rate for diversity order 2 compared to traditional

SCMA. For further analysis in another simulation set, the diversity order is set to 16, and the results are shown in Figure 4.7 and Figure 4.8.

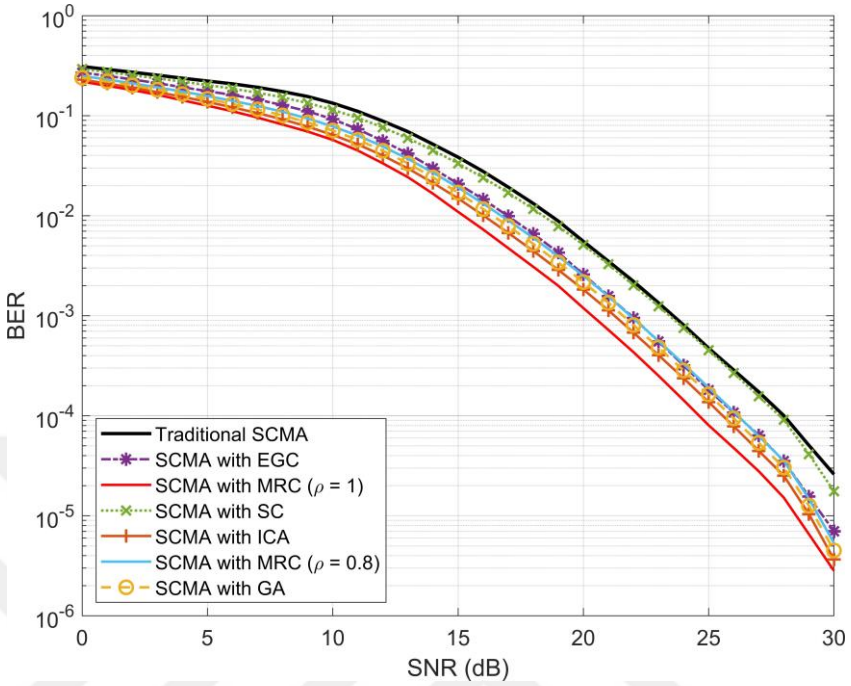


Figure 4.7: Bit-Error Rate Performance Comparison for EGC, MRC, SC, ICA, and GA for diversity order 16.

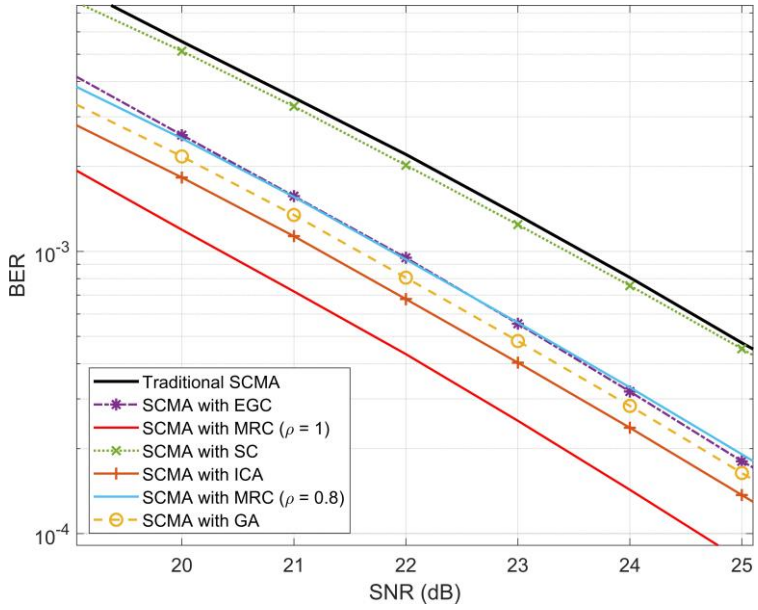


Figure 4.8: Zoomed-in version of Figure 4.7 for BER of $10^{-3}$.

Figure 4.7 and Figure 4.8 show that when ICA is deployed under imperfect channel conditions, there is a performance gain of 2.3 dB when compared to traditional SCMA. It is also shown that compared to the method used in [52] (EGC), the gain is 0.7 dB. It seems that the optimal outcome is achieved when the channel is accurately estimated and MRC is obtained. Although ICA falls short of the optimum MRC by up to 0.8 dB, it is much better than MRC with $\rho = 0.8$, which falls short by around 1.5 dB.

# 5. FURTHER RESULTS

In this chapter, further results obtained during the study of this PhD thesis are given. These results are presented to support the main work. The initial study for NOMA in Terahertz communication systems is in the first section. In the second section, a new opportunistic diversity allocation method is presented.

## 5.1 NOMA in Terahertz Communication Systems

With the introduction of new technologies such as virtual reality and 3D holograms, the need for increased data transfer speed is growing. Although several techniques are introduced to increase data transfer speed, the bandwidth increase is inevitable.

The first alternative solution to satisfy the data speed demand is millimeter-wave (mmWave) communications. 5G offers two frequency bands, 28 GHz and 60 GHz, as commercial mmWave bands [53]. With the mmWave band, it is expected to have an X data rate, and this will enable various applications; however, it still does not fully fulfill the need.

Another alternative is free space optical (FSO) communication networks, which use infrared frequencies [54]. Since this is a frequency between 300 GHz and 400 THz, the effect of the atmosphere on signal propagation is detrimental [55]. Also, due to the insufficiency of the current technology, the required receiver design is very challenging, making it difficult to achieve the necessary data rates.

The third alternative is Terahertz (THz) communication. The THz band is usually referred to the band between 100 GHz and 1 THz [56]. Between these frequencies, it is expected to have enough bandwidth to reach the desired data rates, yet the signal propagation is not as vulnerable as in FSO. There are several challenges of

THz communication as:

- Highly frequency-selective path loss causes the signal to deteriorate after short distances,
- Multi-path channel gains are almost non-existent,
- Traditional MIMO systems are not possible. Line-of-sight communication is needed.

Examination of the NOMA usage under the mentioned challenges in THz communication is studied in Ü lgen et al. [57]. The following subsections provide the system, the proposed link adaptation algorithm, and the computer simulation results for the proposed model.

### 5.1.1 System Model

In this subsection, the system model of NOMA in THz communication is given. Transmission is assumed to be Time Division Duplex mode downlink, and uplink is not considered. To compare the results obtained with OMA results, OMA results are obtained as in Kokkoniemi et al. [58].

Channel coefficients, h(k), are assumed to follow zero means Gaussian with variance that models the path loss. In addition to the free space path loss, atmospheric absorption is added in THz communication to calculate the total path loss. The total path loss is calculated as

$$PL(f, d, \mu) = \exp(-d(\sum_{i=1}^{4} y_i(f, \mu) + g(f))), \quad (5.1)$$

where f is the operation frequency in Hertz, d is the distance between transmitter and receiver, y and g are the atmospheric absorption elements. $\mu$ is calculated as

$$\mu = \frac{\phi}{100} \frac{p_w(T, p)}{p}, \quad (5.2)$$

where $\phi$ is the relative humidity, and p is the pressure. Here, $p_w$ denotes the function of the water vapor partial pressure for the given temperature T and pressure p.

In the Thz communication band, there are some frequencies called atmospheric absorption lines. At these frequencies, communication is almost impossible. The lines are also mentioned in (5.1) as $y_1, \ldots, y_4$. The calculation of $y_i$ where $i = 1, 2, 3, 4$ is given as

$$y_1(f,\mu) = \frac{A(\mu)}{B(\mu) + (\frac{f}{100c} - p_1)^2}, \tag{5.3}$$

$$y_2(f,\mu) = \frac{C(\mu)}{D(\mu) + (\frac{f}{100c} - p_2)^2}, \tag{5.4}$$

$$y_3(f,\mu) = \frac{E(\mu)}{F(\mu) + (\frac{f}{100c} - p_3)^2}, \tag{5.5}$$

$$y_4(f,\mu) = \frac{G(\mu)}{H(\mu) + (\frac{f}{100c} - p_4)^2}. \tag{5.6}$$

Also g of the (5.1) is shown as

$$g(f,\mu) = \frac{\mu}{0.0157}(q_1 f^4 + q_2 f^3 + q_3 f^2 + q_4 f + q_5). \tag{5.7}$$

The variables to define $y_i$ above are given as follows: $A(\mu) = 0.2251\mu(0.1314\mu + 0.0297)$, $B(\mu) = (0.4127\mu + 0.0932)^2$, $C(\mu) = 2.053\mu(0.1717\mu + 0.0306)$, $D(\mu) = (0.5394\mu + 0.0961)^2$, $E(\mu) = 0.177\mu(0.0832\mu + 0.0213)$, $F(\mu) = (0.2615\mu + 0.0668)^2$, $G(\mu) = 2.146\mu(0.1206\mu + 0.0277)$, $H(\mu) = (0.3789\mu + 0.0871)^2$, $p_1 = 10.84\text{cm}^{-1}$, $p_2 = 12.68\text{cm}^{-1}$, $p_3 = 14.65\text{cm}^{-1}$, and $p_4 = 14.94\text{cm}^{-1}$. The variables in the definition of g are given as $q_1 = 8.495\times10^{-48}$, $q_2 = -9.932\times10^{-36}$, $q_3 = 4.336\times10^{-24}$, $q_4 = -8.33 \times 10^{-13}$, and $q_5 = 5.953 \times 10^{-2}$.

With the definitions of absorption lines, Figure 5.1 shows the path gain between 200 GHz and 500 GHz with various distances between receiver and transmitter. It is shown that the absorption lines are at 325 GHz, 380 GHz, 439 GHz, and 448 GHz.

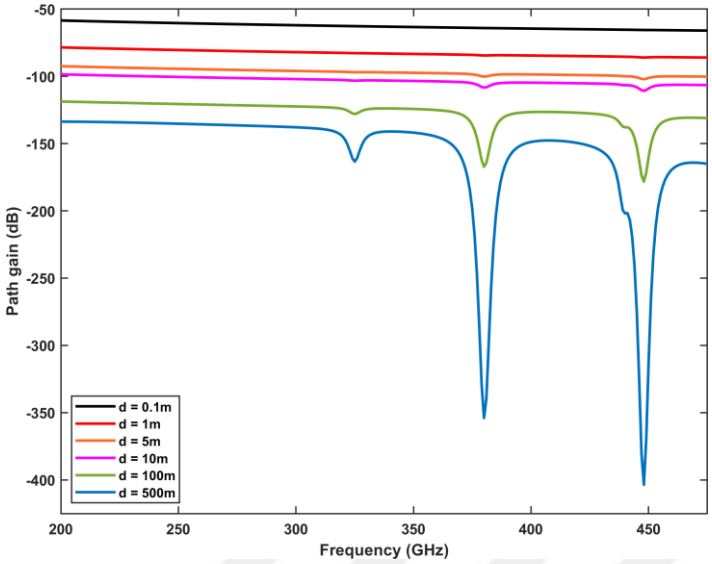


Figure 5.1: Path gains for various distances between receiver and transmitter for the frequencies between 200 GHz and 500 GHz.

It is assumed that the model has two users connected to one access point, and each user has communication distances $d_1$ and $d_2$ from the access point. The operating frequency is 350 GHz, and the communication occurs with line-of-sight without any multi-path fading. Two scenarios are considered in this work. In the first scenario, it is assumed that both users are at the same distance to the access point ($d_1 = d_2$). In scenario 2, the users are at different distances. For each scenario, NOMA and OMA results are compared.

Similar algorithms are implemented to distinguish the performance differences between NOMA and OMA. The adaptive modulation order selection method is the link adaptation method chosen for OMA [59]. To determine the appropriate modulation order in the proposed algorithm, we need to follow these steps:

1. Calculate the available transmission bandwidth.
2. Determine the number of sub-carriers for the given bandwidth.
3. Calculate the instantaneous path loss for the given sub-carriers to identify virtual sub-carriers.

4. Allocate power to the non-virtual sub-carriers.
5. Determine the achievable SNR with the given power of the sub-carriers.
6. Select the suitable modulation order.

For the first step, available transmission bandwidth is given as

$$B(d) = f_c^h - \Delta f_h - (f_c^l + \Delta f_l) \tag{5.8}$$

where $d$ is the transmission distance, $f_c^h$ is the high absorption line central frequency, and $f_c^l$ is the low absorption line central frequency. To calculate $\Delta f_h$ and $\Delta f_l$, the method proposed in Boulogeorgos et al. [59] is utilized.

The number of selected sub-carriers is shown as $N_{sub} = 128$ for both OMA and NOMA. In each sub-carrier, the instantaneous path loss is calculated. The calculated path loss is then compared with the path loss threshold $PL_{th}$. The threshold is given as

$$PL_{th} = \frac{P_t}{N_{sub}} + G_t + G_r - (\gamma_t + P_n) \tag{5.9}$$

where $P_t$ is the total transmission power, $G_t$ is the antenna gain for the transmitter, $G_r$ is the antenna gain for the receiver, $gamma_t$ is the average SNR, and $P_n$ is the noise power.

The sub-carriers with higher path loss values than the threshold are selected as virtual sub-carriers and are excluded from the next steps.

In NOMA, total power $P_t$ is shared between two users as follows.

$$\begin{matrix} p_1 = p_1' \\ p_1' + p_2, \end{matrix} \tag{5.10}$$

where

$$p_i' = \frac{U_i(d)}{r_{max}.} \tag{5.11}$$

Here $p_i$ is the power allocated for user $i$, $U_i(d)$ is the user $i$'s distance from the access point, and $r_{max}$ is the maximum communication distance allowed for the BER

requirement selected. In this case, the second user's power becomes $p_2 = P_t - p_1$. It is assumed that perfect SIC is applied in this work.

After the SNR calculations for non-virtual sub-carrier k, the modulation order is set for the required BER $R_{BER}$ as

$$M_k \leq \frac{2\gamma_k}{3} \frac{1}{(1 - \frac{2R_{BER}}{\alpha})^2} - 1 + 1, \tag{5.12}$$

where

$$a = \begin{cases} 1, & M_k = 4 \\ \frac{4}{\log_2(M_k)}, & M_k > 4. \end{cases} \tag{5.13}$$

### 5.1.2 Simulation Results

In this subsection, computer simulation results for the defined model are given. Atmospheric pressure is set as 101325 Pascals (1 atmosphere), humidity is 50%, and temperature is set to 23 degrees Celcius. The access point's maximum transmission power is 10 dBm, and antenna gains are 45 dB for both transmission and receiver. The absorption loss tolerance is 1 dB, and the BER requirement is $10^{-5}$.

Figure 5.2 shows the data rates for scenario 1, where two users are equally distant from the access point. It is observed that OMA performs poorly compared to NOMA for all cases of 0.1m, 1m, and 10m; however, when NOMA performs two times better for 0.1m and 1m, in 10m, the performance of NOMA triples OMA performance.

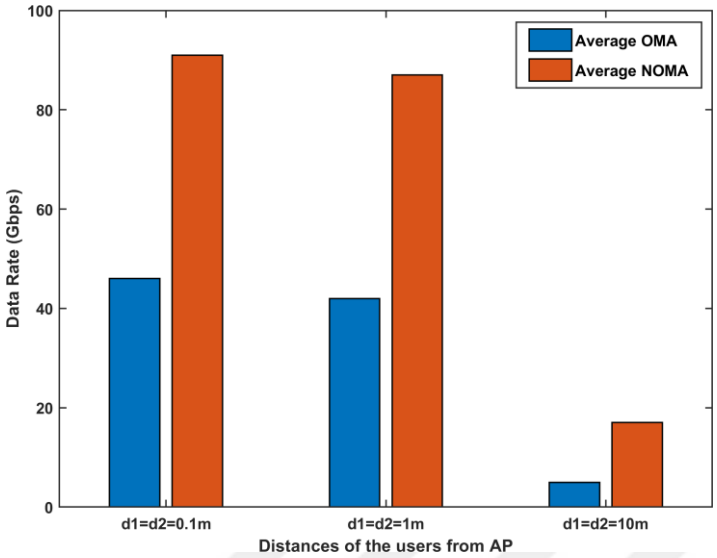


Figure 5.2: Average data rates of OMA and NOMA for various distances between access point and users in Scenario 1.

In scenario 2, the distances of the users are set as 0.1m and 1m for case 1, and 1m and 10m for case 2. In 1000 simulation instances, the minimum, maximum, and average data rates achieved are shown in Figure 5.3. It is demonstrated that NOMA doubles the results for both cases.

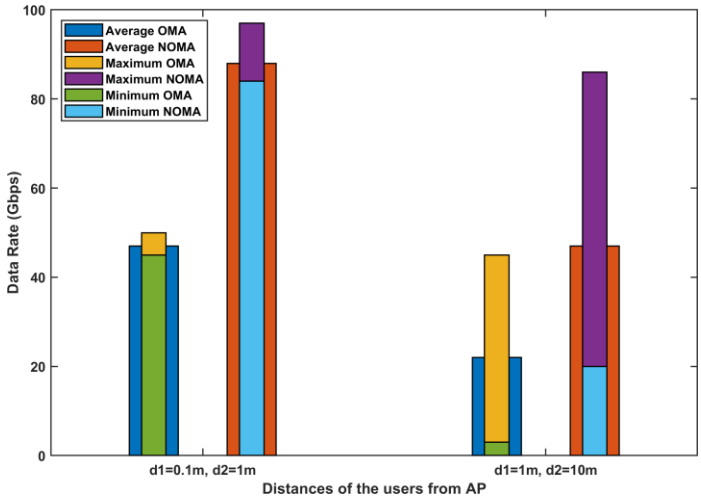


Figure 5.3: Average data rates of OMA and NOMA for various distances between access point and users in Scenario 2.

## 5.2 Opportunistic Diversity Allocation

In this section, an extension of the mainly proposed model is presented. In the proposed model, it is assumed that the spreading factor and repetition factor are fixed. However, it is possible to dynamically adjust these values and create the desired gains in terms of data rate. In the next subsections the system model and computer simulation results are given.

### 5.2.1 System Model

It is shown in the earlier chapters that implementing time-spreading and repetitive transmission provides BER performance increase for SCMA. However, it is possible to adjust the system parameters to increase the data rate while keeping the BER performance at an adequate level. The dynamic adjustment of the parameters, or as it is called in this work, opportunistic diversity allocation can provide the desired results.

Dynamic parameter adjustment is widely used in wireless communication. One of the examples is the dynamic modulation scaling [60]. In this technique, the modulation order of the transmitted signal is dynamically adjusted according to the channel state. This way, more robust communication links are obtained without interrupting the whole communication despite a performance loss overall. Another technique is dynamic frequency/channel allocation [61]. Based on the required gain, frequencies might be dynamically allocated to the users or reallocated if needed. Similar to the given examples, in the time domain, the resources can be allocated dynamically.

Assume there are two transmissions to occur in the mainly proposed model. Assume the spreading factor is set to 4 as well as the repetition factor. Without considering the channel state information, the transmission occurs with the same repetition number. However, if the channel state information is considered, the number of repetitions of the given transmission might be increased or decreased. Figure 5.4

pictures the two different conditions where, in the first one, the repetition factor is reduced to 2, while in the second, it is raised to 5.

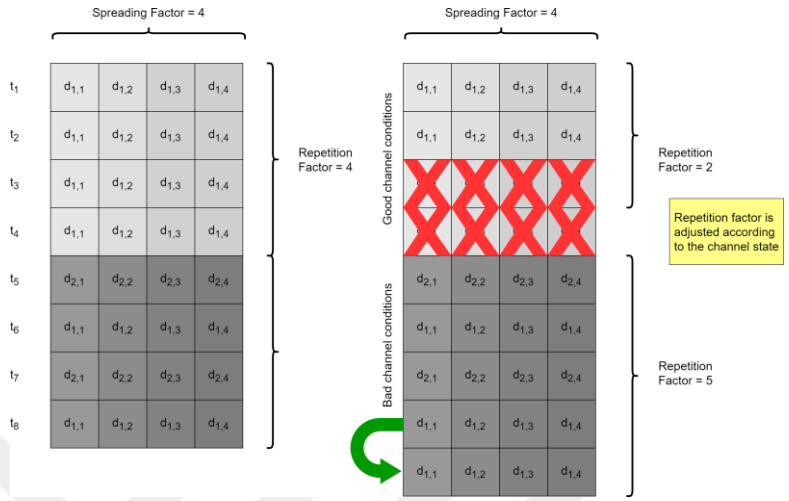


Figure 5.4: Opportunistic adjustment of the repetition factor according to the channel conditions.

Channel state thresholds are introduced to decide whether to increase or decrease the number of repetitions. The overall model is explained in the following paragraphs.

First of all, decision metric M is defined as follows

$$M = \alpha.\gamma_{norm} + \beta.h_{avg-norm} \tag{5.14}$$

where $\gamma_{norm}$ is normalized SNR, $h_{avg-norm}$ is the normalized average channel gain, $\alpha$ is the weighting factor for SNR and $\beta$ is the weighting factor for the channel gain. The threshold is calculated then as

$$R(M) = \begin{cases} R-1, & M > T_1 \\ R, & T_2 < M \leq T_1 \\ R+1, & M \leq T_2 \end{cases} \tag{5.15}$$

where $T_1$ and $T_2$ are the low and high thresholds for adjustment decisions.

### 5.2.2 Simulation Results

In this subsection, computer simulation results are provided for the proposed model. For simulations, it is assumed that the initial setup consists of 4 repetitions and 4 spreading. Three different scenarios are considered to decide the threshold. In the first one, $\alpha$ and $\beta$ are both selected as 0.5. The second scenario is where $\alpha$ is 0.25 and $\beta$ is 0.75, and in the third scenario $\alpha$ is 0.75 and $\beta$ is 0.25. Thresholds of $T_1$ and $T_2$ are selected as 0.33 and 0.67. Figure 5.5 depicts the first scenario.

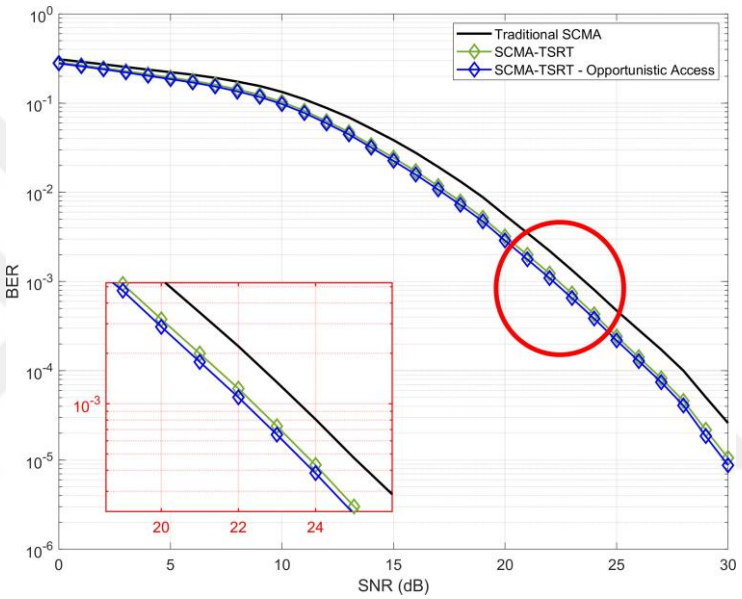


Figure 5.5: BER for SCMA-TSRT vs Opportunistic Access for Spreading factor 4 and $\alpha = 0.5$, $\beta = 0.5$.

It is shown in the figure that, opportunistic access with $\alpha = 0.5$ and $\beta = 0.5$ performs negligibly better in terms of BER. The second scenario is shown in Figure 5.6.

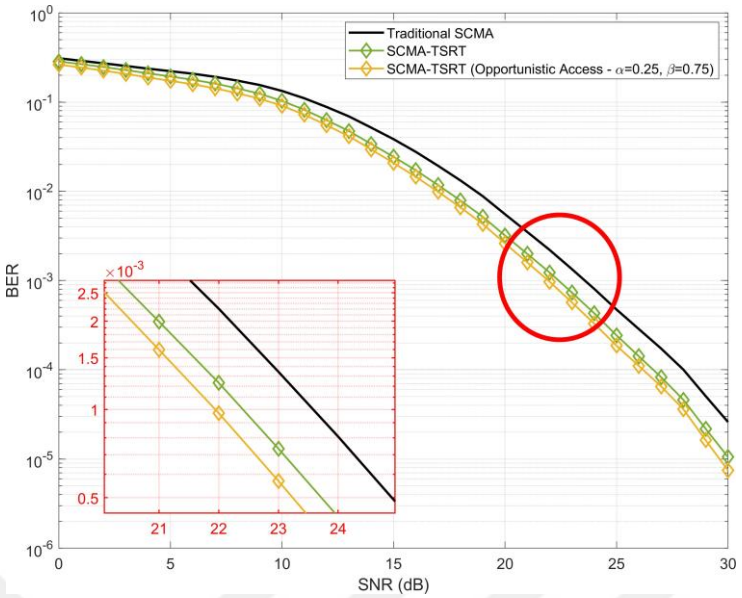


Figure 5.6: BER for SCMA-TSRT vs Opportunistic Access for Spreading factor 4 and α = 0.25, β = 0.75.

Figure 5.6 shows this scenario also performs better than the proposed SCMA-TSRT. The last scenario is shown in Figure 5.7.

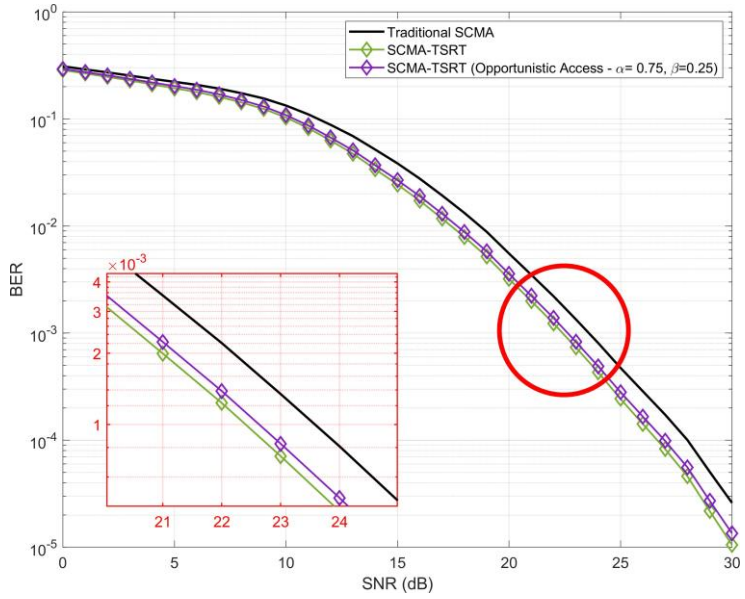


Figure 5.7: BER for SCMA-TSRT vs Opportunistic Access for Spreading factor 4 and α = 0.75, β = 0.25.

In all figures, opportunistic access performs similarly to the SCMA-TSRT. However, the data rates are expected to change. Figure 5.8 shows the data rates for all scenarios while SCMA-TSRT is assumed to have a data rate of 10000 bits per second.

The results show that in the opportunistic access scenarios while keeping the BER performance similar, the overall data rate is increased. For the scenario of $\alpha = 0.25$ and $\beta = 0.75$, the data rate is increased around 15%. In the other scenarios, the results vary from 5% to 10%.

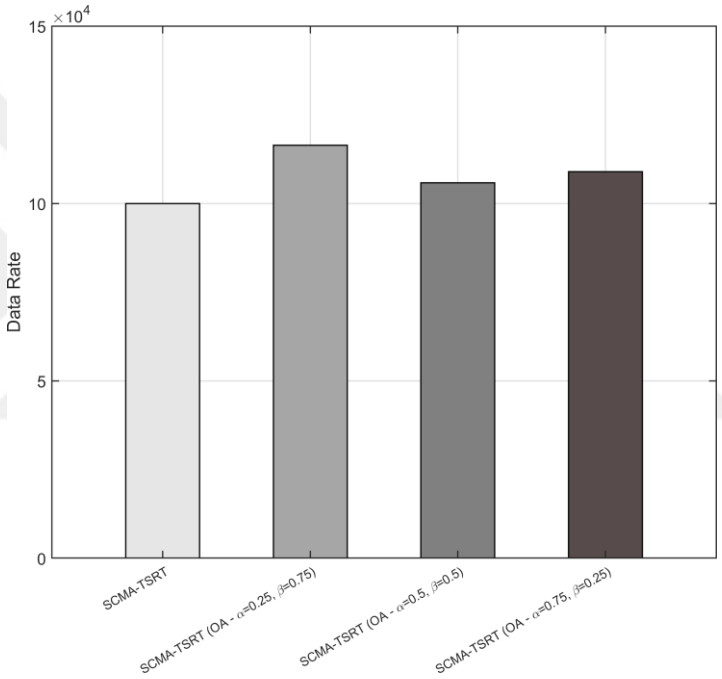


Figure 5.8: Data Rate results for SCMA-TSRT vs Opportunistic Access for Spreading factor 4.

# 6. CONCLUSION AND DISCUSSION

In this thesis, a novel multiple-access technique is introduced that uses Sparse Code Multiple Access as the basis and uses additional techniques such as time-spreading and repetitive transmission. This new technique is called Sparse Code Multiple Access, with time-spreading and repetitive transmission, in short, SCMA-TSRT. Accordingly, mathematical analysis with upper-bound results and computer simulation results for BER performance are given. Other diversity techniques are discussed in further sections. It is shown that the newly proposed model provides up to 3 dB under certain conditions. In the following sections, firstly, the summary of contributions is given, and then future research is discussed.

## 6.1 Summary of Contributions

While discussing the diversity techniques for sparse code multiple access, the main focus of the thesis is the newly introduced SCMA-TSRT technique. During the thesis, the following topics are examined and presented.

- Initially, the key concepts of the thesis are introduced. Non-orthogonal multiple access is explained, and the key diversity techniques are introduced to lay the groundwork for the later topics in the thesis.

- System model of the traditional sparse code multiple access is given and explained in detail. Transmitter and receiver models are shown, and the block diagrams are given.

- Message passing algorithm and maximum-likelihood detection techniques are given to show the in-depth decoding process of an SCMA receiver.

- Time-spreading integration with a mathematical background and computer simulations is presented. The aim is to increase the overall system throughput by increasing the number of orthogonal transmission streams in the system. Although the proposed method increases the throughput, it is shown that the increased number of spreading factor leads to a worsened bit-error-rate performance.

- Repetitive transmission is introduced later. The aim is to increase the overall BER performance of the system. It is shown with the computer simulations and mathematical model that an increased number of repetitive transmissions increases the BER performance. However, this leads to a decreased overall throughput.

- SCMA-TSRT is introduced by combining time-spreading and repetitive transmission to counter-balance each other with strengths and weaknesses. The mathematical analysis is given with upper-bound results. Computer simulations show that SCMA-TSRT is superior to SCMA under certain conditions for the same energy-per-bit. SCMA-TSRT provides up to 1.6 dB BER performance gain.

- Complexity analysis for the proposed model is given by the numbers of additions, multiplications, and exponentials.

- For the signal combining, traditional diversity combining techniques are introduced. Equal gain combining, selection combining, and maximum ratio combining are considered, and received signal equations are given.

- Two meta-heuristic diversity combining techniques are introduced: Genetic algorithm and imperialist competitive algorithm. Both of the techniques are explained in detail.

- Computer simulation results are given for various scenarios with both traditional and meta-heuristic diversity combining techniques. It is shown that using MRC with SCMA-TSRT provides up to 3 dB BER performance gain.

- NOMA results for Terahertz communication networks are given. It is shown that NOMA performs better than OMA in high-frequency channels.

- A novel opportunistic access method is proposed with a dynamic repetition factor. It is shown that data rates can be increased up to 15% for specific scenarios.

### 6.2 Future Research

By considering the contributions of this thesis, several different future research areas can be evaluated. This will further expand and enhance the work and the model proposed as SCMA-TSRT.

Firstly, the implementation of advanced machine learning algorithms is one of the promising development directions. Deep learning or reinforcement learning might be used to improve the decoding performance of the MPA for SCMA-TSRT. In addition, hybrid decoding methods can be implemented to decrease complexity.

The optimization of time-spreading strategies also plays an important role in future research plans. Dynamic resource allocation strategies based on real-time channel conditions for time-spreading would provide an increased BER performance. Similarly, increasing the load of the system might result in a trade-off for increased throughput into a fairly decreased BER. Also, instead of using OVSF, different time chip sequences can be used to improve the BER performance.

Repetitive transmission techniques are another area of improvement for the SCMA-TSRT model. Optimization of repetition patterns, especially by selecting evolved repetition schemes, is a significant research area. Integrating the right schemes in-

creases throughput even without sacrificing BER performance. This way robustness of the SCMA-TSRT might be provided even in high fading channels.

Even though the traditional diversity combining techniques and meta-heuristic algorithms are introduced in this thesis, there are many other diversity combining techniques in literature to be considered. Hybrid models or artificial intelligence-based diversity-combining techniques would allow for the improvement of the novelty of the model even further.

Moreover, the complexity analysis given for the SCMA-TSRT can be extended, and Big-O notation analysis can be introduced. Also, the complexity of the advanced diversity techniques implemented model can be evaluated. This would bring an overlook for the future industrial applications.

Last of all, the computer simulations might be verified with the other state-of-the-art models based on SCMA. Furthermore, different codebooks might be considered to expand the details of the model.

Based on the information listed above, the research directions to be pursued can be increased. SCMA is an important technique for realizing the goals of next-generation communication networks.

# BIBLIOGRAPHY


[1] X. Zhang, H. Qi, X. Zhang and L. Han, ”Spectral Efficiency Improvement and Power Control Optimization of Massive MIMO Networks,” in IEEE Access, vol. 9, pp. 11523-11532, 2021.

[2] H. Nikopour and H. Baligh, ”Sparse code multiple access,” 2013 IEEE 24th Annual International Symposium on Personal, Indoor, and Mobile Radio Communications (PIMRC), London, UK, 2013, pp. 332-336.

[3] Higuchi, K., and Benjebbour, A. (2015). Non-orthogonal Multiple Access (NOMA) with Successive Interference Cancellation for Future Radio Access. IEICE Trans. Commun., 98-B, 403-414.

[4] Moltafet, M., Yamchi, N.M., Javan, M.R., and Azmi, P. (2017). Comparison Study Between PD-NOMA and SCMA. IEEE Transactions on Vehicular Technology, 67, 1830-1834.

[5] Liu, Z., and Yang, L. (2020). Sparse or Dense: A Comparative Study of Code-Domain NOMA Systems. IEEE Transactions on Wireless Communications, 20, 4768-4780.

[6] Moltafet, M., Mokari, N., Javan, M.R., and Azmi, P. (2017). Comparison Study between NOMA and SCMA. ArXiv, abs/1702.01389.

[7] Nikopour, H., Yi, E., Bayesteh, A., Au, K., Hawryluck, M., Baligh, H., and Ma, J. (2014). SCMA for downlink multiple access of 5G wireless networks. 2014 IEEE Global Communications Conference, 3940-3945.

[8] Meriem, A., Anas, H., Adnane, L., and Mounir, A. (2022). SCMA Codebook Design Based on a 16 Star-QAM with MED Maximization. ITM Web of Conferences.

[9] Mardinata, V.A., Kurniawan, D., and Armi, N. (2021). Impact of Overloading Factor on MIMO–SCMA Systems. 2021 International Conference on Radar, Antenna, Microwave, Electronics, and Telecommunications (ICRAMET), 95-98.

[10] Cheraghy, M., and Soltanpour, M. (2022). SER Performance of SCMA Networks with Randomly Distributed Users. 2022 IEEE/CIC International Conference on Communications in China (ICCC), 49-52.

[11] Ali, M.S., Tabassum, H., and Hossain, E. (2016). Dynamic User Clustering and

Power Allocation for Uplink and Downlink Non-Orthogonal Multiple Access (NOMA) Systems. IEEE Access, 4, 6325-6343.

[12] Zhu, L., Zhang, J., Xiao, Z., Cao, X., and Wu, D.O. (2019). Optimal User Pairing for Downlink Non-Orthogonal Multiple Access (NOMA). IEEE Wireless Communications Letters, 8, 328-331.

[13] Zeng, M., Li, X., Li, G., Hao, W., and Dobre, O.A. (2020). Sum Rate Maximization for IRS-Assisted Uplink NOMA. IEEE Communications Letters, 25, 234-238.

[14] Khan, W.U., Jameel, F., Ristaniemi, T., Khan, S., Sidhu, G.A., and Liu, J. (2020). Joint Spectral and Energy Efficiency Optimization for Downlink NOMA Networks. IEEE Transactions on Cognitive Communications and Networking, 6, 645-656.

[15] Taherzadeh, M., Nikopour, H., Bayesteh, A., and Baligh, H. (2014). SCMA Codebook Design. 2014 IEEE 80th Vehicular Technology Conference (VTC2014-Fall), 1-5.

[16] Hoshyar, R., Wathan, F.P., and Tafazolli, R. (2008). Novel Low-Density Signature for Synchronous CDMA Systems Over AWGN Channel. IEEE Transactions on Signal Processing, 56, 1616-1626.

[17] Yuan, Z., Yu, G., Li, W., Yuan, Y., Wang, X., and Xu, J. (2016). Multi-User Shared Access for Internet of Things. 2016 IEEE 83rd Vehicular Technology Conference (VTC Spring), 1-5.

[18] Dai, X., Chen, S., Sun, S., Kang, S., Wang, Y., Shen, Z., and Xu, J. (2014). Successive interference cancelation amenable multiple access (SAMA) for future wireless communications. 2014 IEEE International Conference on Communication Systems, 222-226.

[19] Hoshyar, R., Razavi, R., and Al-Imari, M. (2010). LDS-OFDM an Efficient Multiple Access Technique. 2010 IEEE 71st Vehicular Technology Conference, 1-5.

[20] Islam, S.M., Avazov, N., Dobre, O.A., and Kwak, K.S. (2016). Power-Domain Non-Orthogonal Multiple Access (NOMA) in 5G Systems: Potentials and Challenges. IEEE Communications Surveys and Tutorials, 19, 721-742.

[21] Tachikawa, W., Suetsuna, A., Wang, M., Yoshii, K., and Shimamoto, S. (2023). Applying PDMA for Ground-HAPS Uplink Network with Hybrid FSO/RF Communication. 2023 IEEE Wireless Communications and Network-

ing Conference (WCNC), 1-6.

[22] Ping, L., Liu, L., Wu, K., and Leung, R.W. (2006). Interleave division multiple-access. IEEE Trans. Wirel. Commun., 5, 938-947.

[23] Hu, S., Yu, B., Qian, C., Xiao, Y., Xiong, Q., Sun, C., and Gao, Y. (2018). Nonorthogonal Interleave-Grid Multiple Access Scheme for Industrial Internet of Things in 5G Network. IEEE Transactions on Industrial Informatics, 14, 5436-5446.

[24] Wang, Q., Zhao, Z., Miao, D., Zhang, Y., Sun, J., Liu, M., and Zhong, Z. (2017). Non-Orthogonal Coded Access for Contention-Based Transmission in 5G. 2017 IEEE 86th Vehicular Technology Conference (VTC-Fall), 1-6.

[25] Matsumoto, A., Miyoshi, K., Uesugi, M., and Kato, O. (2001). A study on time domain spreading for OFCDM. The 5th International Symposium on Wireless Personal Multimedia Communications, 2, 725-728 vol.2.

[26] Viterbi, A.J. (1995). CDMA: Principles of Spread Spectrum Communication.

[27] Moose, P.H. (1994). A technique for orthogonal frequency division multiplexing frequency offset correction. IEEE Trans. Commun., 42, 2908-2914.

[28] Vikas, V., Rajesh, A., Deka, K., and Sharma, S.K. (2022). A Comprehensive Technique to Design SCMA Codebooks. IEEE Communications Letters, 26, 1735-1739.

[29] Bao, J., Ma, Z., Xiao, M., and Zhu, Z. (2016). Error Performance of Sparse Code Multiple Access Networks with Joint ML Detection. 2016 IEEE 83rd Vehicular Technology Conference (VTC Spring), 1-5.

[30] Klimentyev, V.P., and Sergienko, A.B. (2016). Detection of SCMA signal with channel estimation error. 2016 18th Conference of Open Innovations Association and Seminar on Information Security and Protection of Information Technology (FRUCT-ISPIT), 106-112.

[31] Damen, M.O., Gamal, H.E., and Caire, G. (2003). On maximum-likelihood detection and the search for the closest lattice point. IEEE Trans. Inf. Theory, 49, 2389-2402.

[32] Chaturvedi, S., Liu, Z., Bohara, V.A., Srivastava, A., and Xiao, P. (2021). A Tutorial to Sparse Code Multiple Access. ArXiv, abs/2105.06860.

[33] Hochwald, B.M., Marzetta, T.L., and Papadias, C.B. (2001). A transmitter diversity scheme for wideband CDMA systems based on space-time spreading. IEEE J. Sel. Areas Commun., 19, 48-60.

[34] Wang, X., and Yang, G. (2021). Time-coding spread-spectrum reconfigurable intelligent surface for secure wireless communication: theory and experiment. Optics express, 29 20, 32031-32041 .

[35] Almeida, A.L., Favier, G., and Mota, J.C. (2009). Space-time spreading-multiplexing for MIMO wireless communication systems using the PARATUCK-2 tensor model. Signal Process., 89, 2103-2116.

[36] Dey, I., Joshi, H., and Marchetti, N. (2021). Space-Time Spreading Aided Distributed MIMO-WSNs. IEEE Communications Letters, 25, 1338-1342.

[37] Nusenu, S.Y., Wang, W., and Basit, A. (2018). Time-Modulated FD-MIMO Array for Integrated Radar and Communication Systems. IEEE Antennas and Wireless Propagation Letters, 17, 1015-1019.

[38] Tseng, Y., and Chao, C. (2001). Code placement and replacement strategies for wideband CDMA OVSF code tree management. GLOBECOM'01. IEEE Global Telecommunications Conference (Cat. No.01CH37270), 1, 562-566 vol.1.

[39] Huang, C., Su, B., Lin, T., and Huang, Y. (2021). Downlink SCMA Codebook Design With Low Error Rate by Maximizing Minimum Euclidean Distance of Superimposed Codewords. IEEE Transactions on Vehicular Technology, 71, 5231-5245.

[40] Yu, L., Lei, X., Fan, P., and Chen, D. (2015). An optimized design of SCMA codebook based on star-QAM signaling constellations. 2015 International Conference on Wireless Communications and Signal Processing (WCSP), 1-5.

[41] Sklar, B. (2012). Rayleigh Fading Channels.

[42] Mansour, M.M. (2006). A Turbo-Decoding Message-Passing Algorithm for Sparse Parity-Check Matrix Codes. IEEE Transactions on Signal Processing, 54, 4376-4392.

[43] Annamalai, A., Tellambura, C., and Bhargava, V.K. (2000). Equal-gain diversity receiver performance in wireless channels. IEEE Trans. Commun., 48, 1732-1745.

[44] Dietrich, F.A., and Utschick, W. (2003). Maximum ratio combining of corre-

lated Rayleigh fading channels with imperfect channel knowledge. IEEE Communications Letters, 7, 419-421.

[45] Kandasamy, K., and Selvaraj, D.M. (2022). SEP of Cooperative NOMA with Selection Combining. 2022 IEEE 19th India Council International Conference (INDICON), 1-6.

[46] Ü lgen, O., Tüfekci, T., Sadi, Y., Erkü cü k, S., Anpalagan, A., Baykas, T., A Comparative Analysis of Diversity Combining Techniques for Repetitive Transmissions in Time Spreading SCMA Systems, Internet Technology Letters, 2024.

[47] Aleksic, D., Krstić, D., Stefanovic, M.C., Petkovic, G., Marjanovic, I., and Radenkovic, D. (2016). Outage Probability Comparison of MRC, EGC and SC Receivers over Short Term Fading Channels. International Journal of Communication, 01.

[48] Akbari, M., and Ghanbarisabagh, M. (2014). A Novel Evolutionary-Based Cooperative Spectrum Sensing Mechanism for Cognitive Radio Networks. Wireless Personal Communications, 79, 1017 - 1030.

[49] Gunjan, Sharma, A.K., and Verma, K. (2022). GA-UCR: Genetic Algorithm Based Unequal Clustering and Routing Protocol for Wireless Sensor Networks. Wireless Personal Communications, 128, 537-558.

[50] Whitley, L.D. (1994). A genetic algorithm tutorial. Statistics and Computing, 4, 65-85.

[51] Atashpaz-Gargari, E., and Lucas, C. (2007). Imperialist competitive algorithm: An algorithm for optimization inspired by imperialistic competition. 2007 IEEE Congress on Evolutionary Computation, 4661-4667.

[52] Ü lgen, O., Tüfekci, T., Sadi, Y., Erkü cü k, S., Anpalagan, A., Baykas, T., Sparse Code Multiple Access with Time Spreading and Repetitive Transmissions, International Journal of Communication Systems, 2024 (Under Review).

[53] Bhargava, Vijay K.. Millimetre wave bands for 5G wireless communications., 2014 International Workshop on High Mobility Wireless Communications (2014).

[54] Khalighi, M.A., and Uysal, M. (2014). Survey on Free Space Optical Communication: A Communication Theory Perspective. IEEE Communications Surveys and Tutorials, 16, 2231-2258.

[55] Sheikh, F., Alissa, M., Zahid, A., Abbasi, Q.H., and Kaiser, T. (2019). Atmospheric Attenuation Analysis in Indoor THz Communication Channels. 2019 IEEE International Symposium on Antennas and Propagation and USNC-URSI Radio Science Meeting, 2137-2138.

[56] Han, C., Wang, Y., Li, Y., Chen, Y., Abbasi, N.A., Kürner, T., and F. Molisch, A. (2021). Terahertz Wireless Channels: A Holistic Survey on Measurement, Modeling, and Analysis. IEEE Communications Surveys Tutorials, 24, 1670-1707.

[57] Ü lgen, O., Erkü çük, S., and Bayka¸s, T. (2020). Non-Orthogonal Multiple Access for Terahertz Communication Networks. 2020 11th IEEE Annual Ubiquitous Computing, Electronics and Mobile Communication Conference (UEMCON).

[58] Kokkoniemi, J., Lehtomäki, J.J., and Juntti, M.J. (2019). Simple Molecular Absorption Loss Model for 200–450 Gigahertz Frequency Band. 2019 European Conference on Networks and Communications (EuCNC), 219-223.

[59] Boulogeorgos, A.A., Papasotiriou, E.N., and Alexiou, A. (2018). A Distance and Bandwidth Dependent Adaptive Modulation Scheme for THz Communications. 2018 IEEE 19th International Workshop on Signal Processing Advances in Wireless Communications (SPAWC), 1-5.

[60] Sheu, T., Chang, K., and Yeh, F. (2017). A Dynamic Allocation Scheme for Resource Blocks Using ARQ Status Reports in LTE Networks. 2017 International Conference on Information, Communication and Engineering (ICICE), 224-227.

[61] Ashraf, M., Hassan, S., Rubab, S., Khan, M.A., Tariq, U., and Kadry, S. (2022). Energy-efficient dynamic channel allocation algorithm in wireless body area network. Environment, Development and Sustainability, 1-17.

# 7. Curriculum Vitae

He received his B.Sc. in 2014 and M.Sc. in 2018 in Electronics Engineering from Kadir Has University. He has worked for several companies, including Huawei, Siemens, and Accenture. Currently, he is continuing his career as a senior standardization researcher at NTT DOCOMO Euro-Labs in Munich, Germany.

Publications for the thesis are listed below:

- Ü lgen, O., Erkü çü k, S., and Bayka¸s, T. (2020). Non-Orthogonal Multiple Access for Terahertz Communication Networks. 2020 11th IEEE Annual Ubiquitous Computing, Electronics and Mobile Communication Conference (UEMCON), 0737-0742.
- Ülgen, O., Tüfekci, T., Sadi, Y., Erkücük, S., Anpalagan, A., Baykas, T., A Comparative Analysis of Diversity Combining Techniques for Repetitive Transmissions in Time Spreading SCMA Systems, Internet Technology Letters, 2024.
- Ülgen, O., Tüfekci, T., Sadi, Y., Erkücük, S., Anpalagan, A., Baykas, T., Sparse Code Multiple Access with Time Spreading and Repetitive Transmissions, International Journal of Communication Systems, 2024 (Under Review).